ANL-6689

Argonne National Laboratory

ZERO-POWER EXPERIMENTS WITH BOILING CORE B-1, BORAX-V

by

BORAX-V Project Staff
Idaho Division

ANL-6689
Reactor Technology
(TID-4500, 21st Ed.)
AEC Research and
Development Report

ARGONNE NATIONAL LABORATORY
9700 South Cass Avenue
Argonne, Illinois 60440

ZERO-POWER EXPERIMENTS WITH BOILING CORE B-1, BORAX-V

by

BORAX-V Project Staff
Idaho Division

Contributors:

R. E. Rice
R. A. Cushman
J. I. Hagen
R. J. Jiacoletti*
A. W. Solbrig, Jr.
W. R. Wallin
E. J. Brooks
D. H. Brown
G. S. Brunson
J. D. Cerchione
C. C. Miles
R. W. Thiel

*University of Wyoming

June 1963

Operated by The University of Chicago
under
Contract W-31-109-eng-38
with the
U. S. Atomic Energy Commission

TABLE OF CONTENTS

TABLE OF CONTENTS

LIST OF FIGURES

LIST OF FIGURES

LIST OF FIGURES

ZERO-POWER EXPERIMENTS WITH BOILING CORE B-1, BORAX-V

by

BORAX-V Project Staff
Idaho Division

I. INTRODUCTION

The primary purposes of the initial boiling-core experiments with BORAX-V were to shake down the reactor and steam plants and to determine certain reactor characteristics before proceeding with the testing of cores with integral nuclear superheaters.

This report covers only the results of the zero-power operation of the initial boiling core, B-1, from room-temperature, atmospheric-pressure conditions to the operating conditions at 489°F and 600 psig. The core characteristics of primary interest which were measured are critical mass, control rod calibrations, excess reactivity, shutdown reactivity margin, reactivity effects of various core components, reactivity effects of temperature and voids, neutron flux and power distributions, and cadmium ratios. In addition, some development and calibration work was done on a rotating oscillator rod.

In the course of the experiments with core B-1, the core was changed several times. The five different basic core loadings have been designated as follows:

Core B-1A - 36 poison rods, old control rods

Core B-1B - 32 poison rods, old control rods

Core B-1B' - 32 poison rods, new control rods

Core B-1C - 34 poison rods, new control rods

Core B-1D - 32 poison rods, new control rods, oscillator, and instrument thimbles

At the conclusion of the zero-power experiments at operating conditions, the available excess reactivity (with the oscillator rod installed) at 489°F and 600 psig, was only about 3.2%. Based on the measured reactivity worth of voids at room temperature and the expectation that void worth would be higher at operating temperature, it was estimated that the rated full power of 20 Mwt probably could not be achieved. Therefore, the planned power operation of core B-1 was cancelled, and core changes were started for core B-2, designed to achieve more available excess reactivity.

To expedite publication of the data contained herein, a detailed analysis of results has not been included in this report, although some comparison with calculated values has been made. In general, no error estimates are included for results in this report.

II. REACTOR DESCRIPTION[1]

The BORAX-V reactor and power-plant equipment are located in two buildings one-half mile from the Control Building. The turbogenerator is located 200 ft from the Reactor Building.

The reactor vessel is a cylinder with ellipsoidal heads, of $5\frac{1}{2}$-ft ID and 16-ft internal height. The core is centered about 4 ft from the vessel bottom. Three separate core configurations can be used: a boiling core without superheater, a boiling core with a centrally located superheater, and a boiling core with a peripherally located superheater.

The boiling core (see Fig. 1) is 24 in. high and has an effective diameter of 39 in. when containing the maximum of sixty $3\frac{7}{8}$-in.-sq fuel assemblies arranged in an 8 x 8 array with corner assemblies missing. Each square cell of four assemblies is surrounded by adjacent control rod channels.

The boiling assemblies are composed of individually removable fuel rods (the number of rods per assembly may vary from 0 to 49) made of UO_2 of 4.95 w/o (design reference is 16.3 g of U^{235} per rod) enrichment with 0.015-in. Type 304 stainless steel cladding. Fuel rods of 9.90 w/o enrichment are used for special experiments. The outside diameter of the rods is 0.375 in. (see Figs. 2 and 3). Poison rods of stainless steel or boron-stainless steel can be substituted for fuel rods for flux flattening and adjustment of excess reactivity. The design of the boron-stainless steel rods is shown in Fig. 4. All the poison rods actually used as part of the loadings for core B-1 were made of boron-stainless steel.

The nine control rods are made of Boral canned in stainless steel. The central and four intermediate control rods are cruciform in shape, and the four outer rods are T-shaped. The control rods are driven from below the reactor vessel, through a linear seal, by motor-driven, lead screw-and-nut mechanisms with solenoid scram latches.

For the initial zero-power operation, fuel rods were loaded into the boiling assemblies manually. A special telescoping handling tool was used to engage the assembly and suspend it from the crane. The assembly was lowered into a core position by operation of the motor-driven crane hoist.

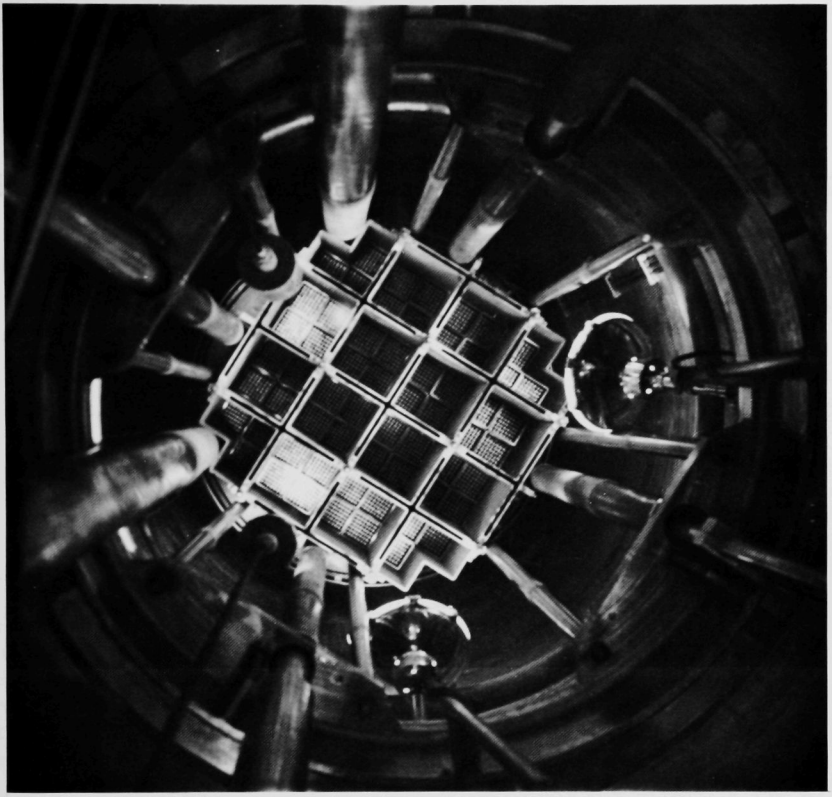

Fig. 1. Boiling Core B-1 of BORAX-V

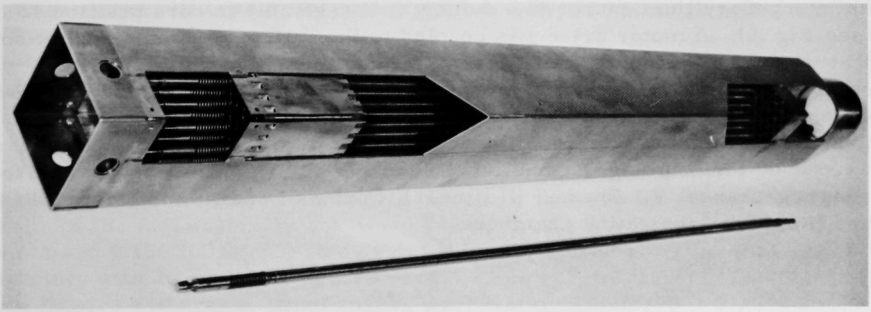

Fig. 2. Fuel Rod and Cutaway Section of Boiling Fuel Assembly of BORAX-V

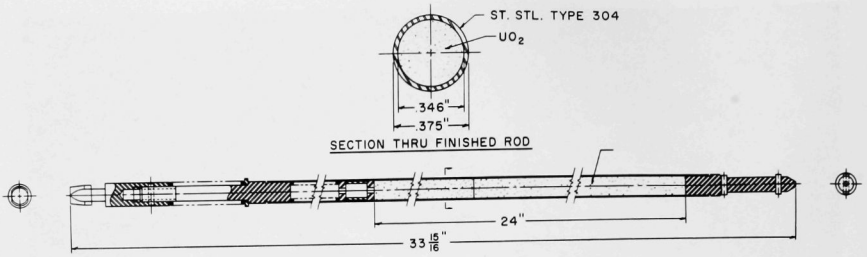

Fig. 3. Boiling Fuel Rod of BORAX-V

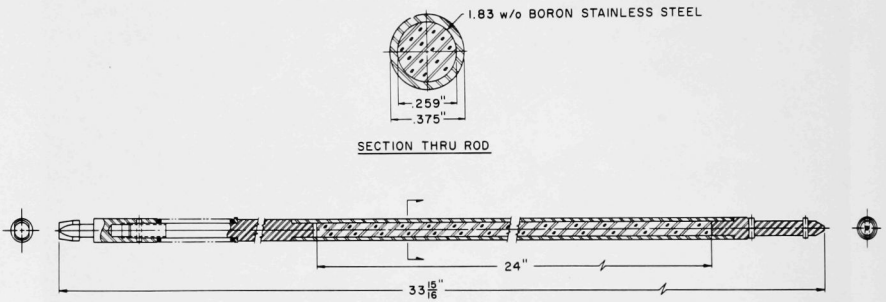

Fig. 4. Boron-Stainless Steel Poison Rod of BORAX-V

III. ROOM-TEMPERATURE EXPERIMENTS

A. Loading to Minimum-critical-mass Core

The reactor was prepared for the first loading by placing an antimony-beryllium source in a dummy fuel assembly in core position 42 (see Fig. 5). A motor drive was coupled to the antimony gamma source so that it could be remotely raised from its position within the beryllium, located at the core midplane, to a position 42 in. above the midplane, thereby essentially stopping production of source neutrons. Neutron counters and ionization chambers were positioned as shown in Fig. 5. Fission chambers were used for counting-channels I, II, and IV. A BF_3 chamber was used for counting-channel V. Channel III (linear), Periods I and II, and Safeties I and II used B^{10} ionization chambers.

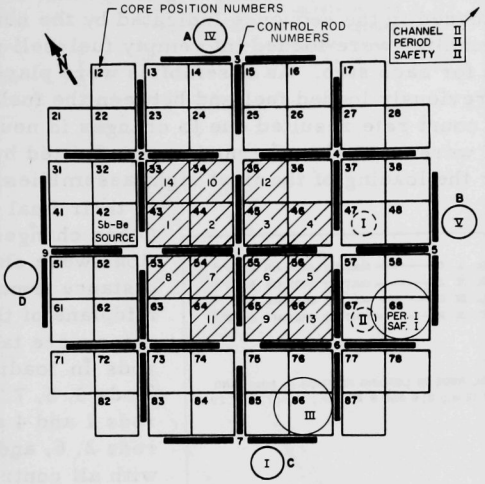

Fig. 5. Minimum-critical-loading Diagram for Core B-1 of BORAX-V

The number of boiling fuel assemblies with 49 fuel rods each, calculated to give a cold clean critical configuration (in a cylindrical geometry) was 11 (539 fuel rods). Critical experiments performed at ZPR-VII showed that 645 fuel rods were required in a clean cylindrical array to produce a critical reactor.(2) Also, 689 ± 4 fuel rods (equivalent to ~14 assemblies) were required to produce a critical slab core loading having 35 fuel rods on the longer side.

Criticality in BORAX-V was achieved with 14 assemblies (686 fuel rods) in the reactor arranged as a square with two opposite corner assemblies removed, as shown in Fig. 5. The significant differences in the measurements with ZPR-VII and BORAX-V may be explained by the differences in lattice geometry due to water in control rod channels and between fuel assemblies, and the presence of more aluminum structure in the BORAX-V reactor.

The BORAX-V boiling fuel assembly uses a 0.5-in. fuel rod spacing within an assembly; however, between assemblies the spacing is 0.916 in., and across the control rod channels the space is 1.896 in. The aluminum walls of the fuel assembly box are 0.062 in. thick, and the aluminum shroud walls are 0.156 in. thick. The ZPR-VII loadings used a 0.5-in. fuel rod spacing, with 20 fuel rod spaces used for control rod fingers. With control rod fingers withdrawn, these spaces were water-filled.

Boiling fuel assemblies, each having forty-nine 4.95-w/o-enriched fuel rods, were loaded in the sequence indicated by the numbers in Fig. 5. Dummy fuel assemblies were loaded into empty fuel-cell positions to maintain fuel location for each step. As assemblies were placed between the source and the previously loaded fuel and between the fuel and the counters, large changes in count rate resulted due to changes in neutron attenuation. Channels I and II were located in the positions indicated by the dashed circles in Fig. 5 for the loading of the first eight assemblies and then moved to their final radial position. Other changes in counter positions were changes in vertical distance from the horizontal midplane of the core. Count rates were taken with control rods in loading position I (rods 3, 5, 7, and 9 at 29 in.; rods 1 and 4 at 12 in.; and rods 2, 6, and 8 at 0 in.) and with all control rods at 29 in. (poison fully removed from the core). Reciprocal count-rate curves are shown in Figs. 6 and 7 for the control rods in loading position I and in the control-rods-withdrawn position, respectively.

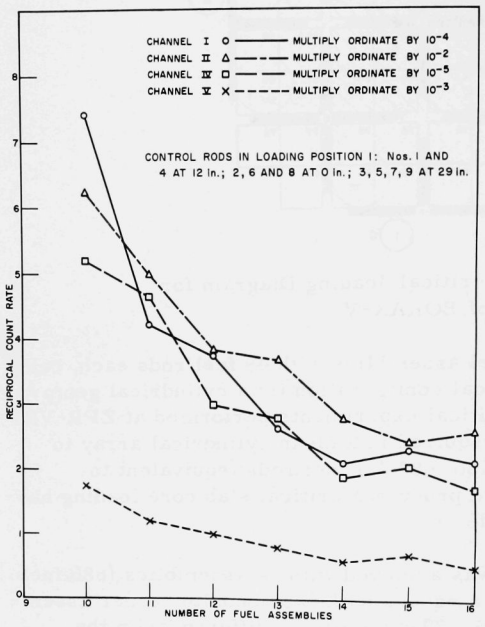

Fig. 6. Approach to Minimum Critical Loading (Control Rods in Loading Position No. 1)

B. Loading to 60-Assembly Core

1. Loading

The objectives of the loading to a 60-assembly core were to produce one which would subsequently be used to develop as much power as possible and to produce a reference to which future superheating cores could be compared. The restriction was adopted that the single-control-rod criticality criterion should be satisfied, i.e., that the reactor should be subcritical with any single control rod fully withdrawn and all eight other rods fully inserted. The number and location of fuel and poison rods were eventually chosen to minimize neutron flux peaks and to satisfy this control criterion.

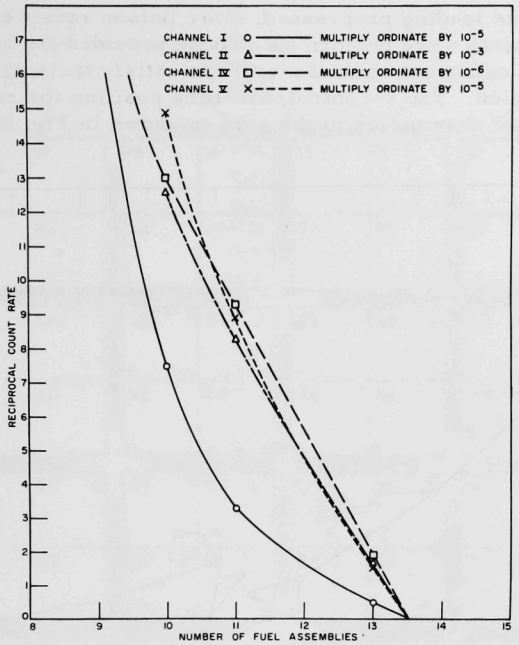

Fig. 7. Approach to Minimum Critical Loading
(All Control Rods at 29 in.)

Counting rates were logged with control rods in loading position I. These were taken to assure that the reactor would be subcritical during the loading of fuel. Counts were also taken with the central rod withdrawn to 29 in., and with the central rod at 29 in. and one intermediate rod partially withdrawn. These counts were taken to enable a prediction of the possibility that the reactor could go critical on the withdrawal of a single control rod alone.

After the initial unpoisoned loading of 14 fuel assemblies, two more assemblies were added and six boron-stainless steel poison rods were installed in the center four assemblies. The neutron source was moved to its permanent thimble outside the core, and the neutron detectors were repositioned to give coverage of the change in multiplication from reactor shutdown, with all control rods inserted, to reactor critical. This change allowed a full fuel loading without further relocation of detectors. The source and detector locations for the remainder of the loadings are shown in Fig. 9.

As the loading progressed, more poison rods were added and critical experiments were performed. These provided the added assurance that there was a sufficient control margin to satisfy the single-control-rod criticality criterion. The 9-control-rod-bank position for reactor criticality vs. number of fuel assemblies in the core is shown in Fig. 8.

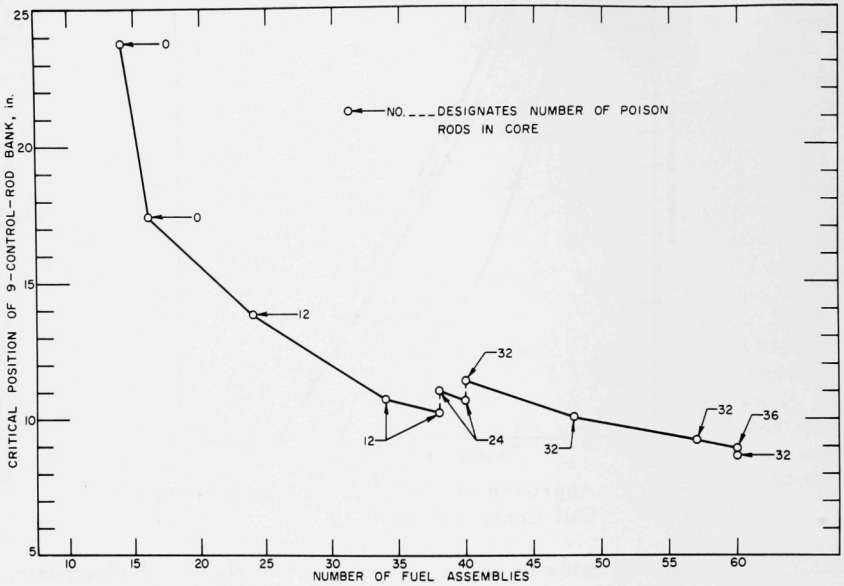

Fig. 8. Critical Approach to Full-size Core B-1

2. Poison-rod Adjustment

Upon reaching the 60-assembly loading with 32 poison rods installed, the reactor was found to be critical upon withdrawal of any one of the intermediate control rods. This condition was changed by the addition of four poison rods, for a total of 36 poison rods, and the relocation of eight others to positions near the intermediate rods. The fully loaded boiling core B-1A and poison-rod location at this time are shown in Fig. 9. This core was used during many of the control rod calibrations, reactivity measurements, and flux-wire irradiations. Boric acid solution was added to the reactor water to permit almost complete withdrawal of the 9-control-rod bank during these measurements.

Later, after boric acid was removed from the reactor water, the poison-rod locations were changed to position the boron-stainless steel rods in the positions of peak flux as determined by the fine-flux distribution

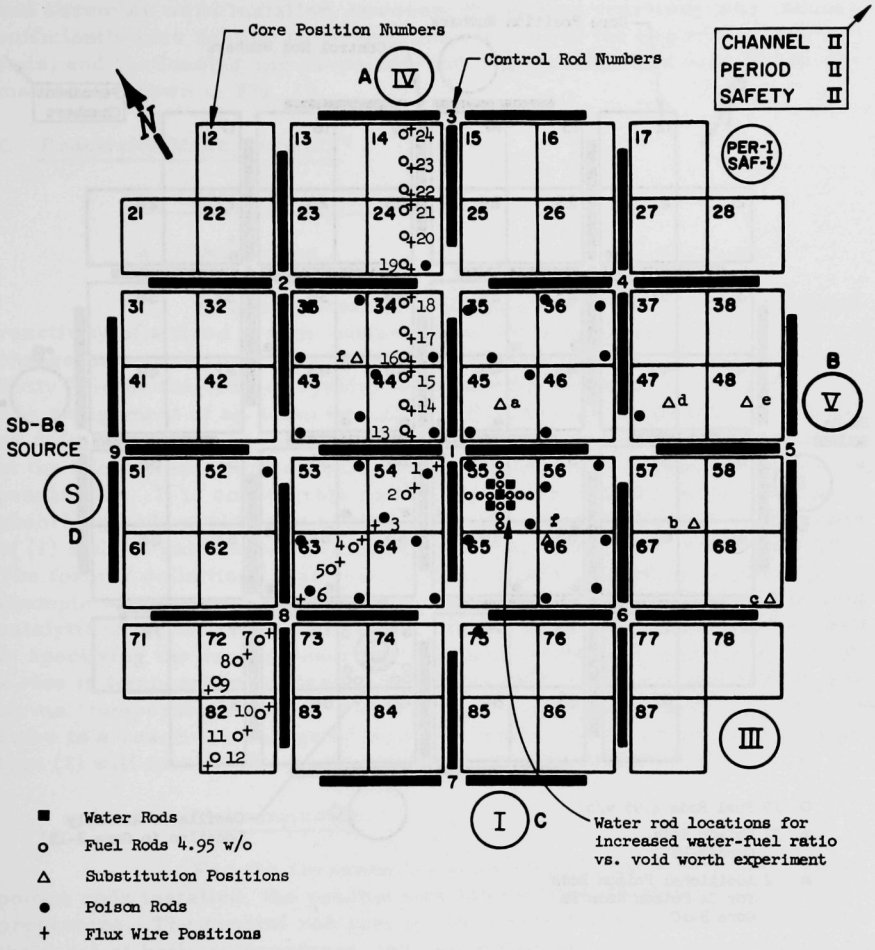

Fig. 9. Experimental Loading Diagram for Core B-1A

measurements. Because poison rods in these locations had a greater negative reactivity effect, it was possible to reduce the number of poison rods to 32 and still not go critical upon the withdrawal of any single control rod, with all other rods inserted. This poison-rod configuration, which is the loading for the boiling core B-1B, is shown in Fig. 10.

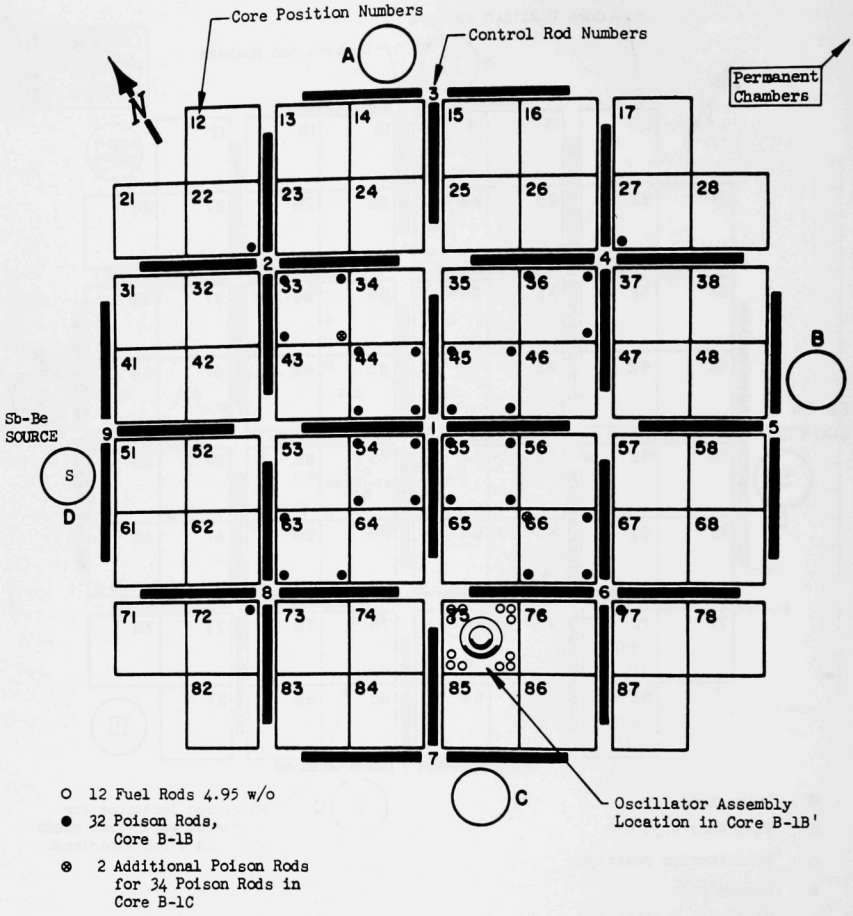

Fig. 10. Poison Rod Locations for Cores B-1B, B-1B', and B-1C

After the above poison-rod manipulations, the original set of control rods was replaced with a new set. These new rods had essentially the same composition as the original set, but minor design improvements and better quality control had been incorporated during fabrication and the rods were subjected to more stringent test (see Section III.C.2.b., New Control Rods). Additional checks for criticality with any single control rod withdrawn indicated a need for two more poison rods, for a total of 34, located as shown in Fig. 10 for core B-1C. When the oscillator rod

and assembly were installed, however, the excess reactivity was reduced sufficiently (see Section III.G) to allow removal of the two added poison rods, and the loading and 32-poison-rod configuration for core B-1B' remained as shown in Fig. 10.

C. Reactivity Measurements*

1. Temperature Effect

a. Definitions

"It is important to distinguish between: (1) the change in reactivity of a fixed system whose temperature is changed, and (2) the net change in excess reactivity available to the system, e.g., the excess reactivity held by the control system, when the temperature is changed... The assignment of an accurate value to the average temperature coefficient as defined in (2) requires a very accurate calibration of the control system at the two extreme temperatures and over the entire region of control rod penetration. It is conceivable that a cold reactor controlled by neutron-absorbing rods could have a negative temperature coefficient in the sense of (1) and yet gain excess available reactivity upon a rise in temperature. The former definition (1) is related to questions of reactor safety, for example whether or not a rise in temperature of the system would be autocatalytic if control rods were left in place. The latter concept (2) is used in specifying the excess reactivity required in the cold reactor to permit a rise in temperature to design conditions."[3] In the present report, the terms "temperature effect," "void effect," "boric acid effect," and the like refer to a reactivity change of type (1). Reference to a reactivity change of type (2) will involve the words "available excess reactivity."

b. Measurements

For the 16-assembly core with six boron-stainless steel poison rods installed, the reactor was heated from 68 to 91°F by electric preheaters. The control rod position for reactor critical was essentially the same at both temperatures, indicating that the overall temperature effect was approximately zero in this temperature range.

For core B-1B, the temperature effect was measured by electrically heating the reactor water from 67 to 105°F, and then cooling, to eliminate air bubbles, until the temperature reached 94°F. The change in reactivity from 67 to 94°F was determined from the change in critical position of the central control rod. The central control rod was calibrated by measuring periods resulting from incremental rod movement. From

---

*Values of reactivity were computed from measured periods by use of the expression on p. 27 of ANL-5800, with $\beta = 0.0071$, $\ell = 3 \times 10^{-5}$ sec, and other parameters for U^{235} from Tables 1-13 of ANL-5800.[4]

these measurements, it is inferred that, had the control rods remained at the position of criticality at 67°F, a reactivity loss of ~0.1% would have occurred upon heating the water to 94°F, which gives a temperature effect of ~-0.004% $\Delta k/k/°F$.

In core B-1A, with the reactor water containing dissolved boric acid in the amount of 18.75 $g(H_3BO_3)/gal(H_2O)$, the temperature was changed from 79 to 112°F and then brought down to 101°F. The temperature difference from 79 to 101°F resulted in a reactivity change of -0.005%. When correction was made for the net change in boric acid concentration due to expansion of the water and the core structure, and for the change in boric acid concentration due to evaporation, the reactivity effect due to this temperature change was essentially zero. The dependence of the boric acid effect upon temperature was neglected. An estimate of this effect is given in Section V. Because of the large corrections required for boric acid displacement, the accuracy of this measurement is questionable.

2. Control Rod Worths

The reactivity worths of control rods were determined by measuring the period produced when the control rod or group of rods was raised slightly above the critical position. Boric acid solution was added in increments to compensate for adjustment of critical positions of the control rods. In this manner, in core B-1A, the control rods were calibrated over a range to the vicinity of 20-22 in.

Attempts to measure the control rod worth by rod-drop tests were unsuccessful because of difficulties in obtaining a satisfactory record of neutron flux. To be able to operate at low power levels and thereby to keep fuel activation at a minimum, the flux-detecting chambers were located in temporary watertight thimbles in the reactor vessel. Dropping control rods produced sufficient vibration to distort the flux record.

a. Original Control Rods

Figure 11 shows the integral reactivity worth ($\int_Z^{26}$ differential worth $(Z')dZ'$, where Z' is the rod position in in.) of all the original control rods in a bank in core B-1A. The differential worth of banked control rods is shown in Fig. 12. The relative differential worth of individual control rods is shown in Fig. 13. The central rod had the greatest worth; its maximum effect was about 0.45% $\Delta k/k/in$. Each intermediate control rod was worth about 57% of the central rod, and each outside rod was worth about 17% of the central rod when small increments were evaluated near the rod-bank position.

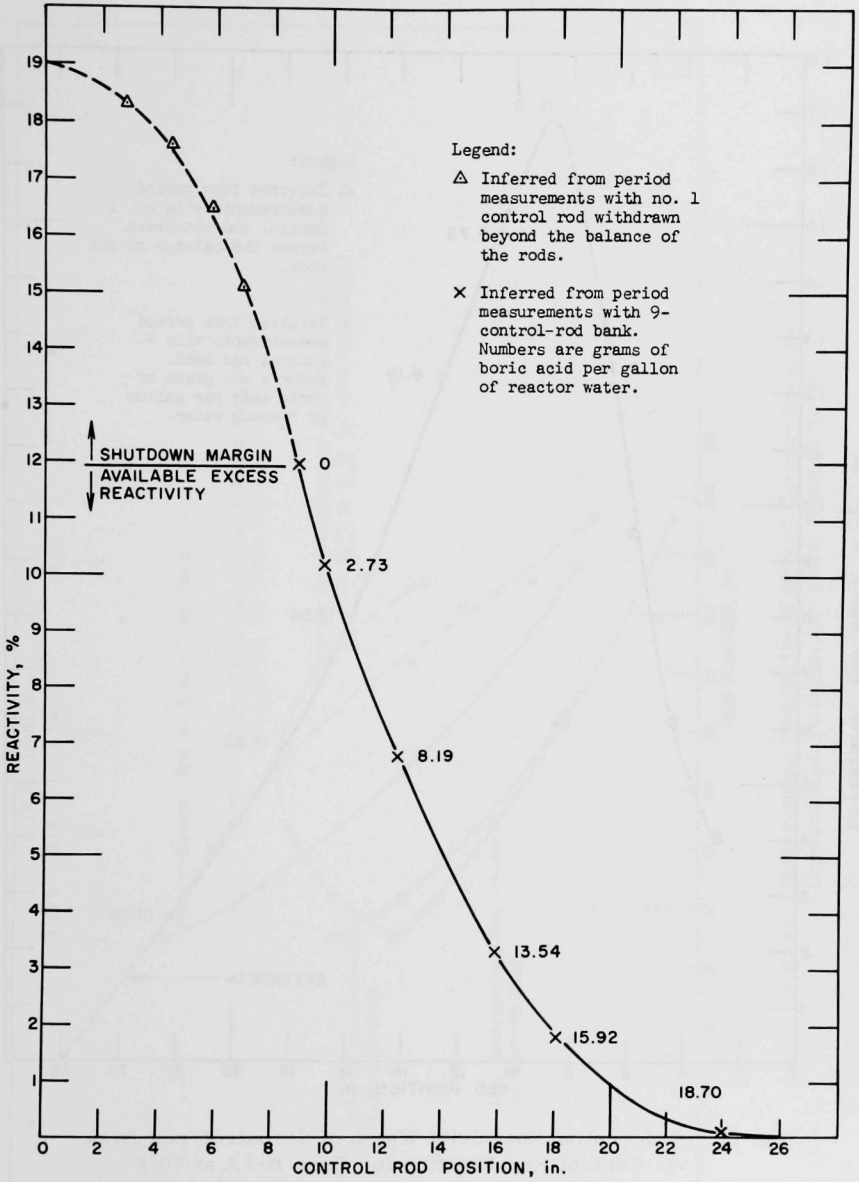

Fig. 11. Reactivity Controlled by 9-control-rod Bank of Core B-1A at 70°F

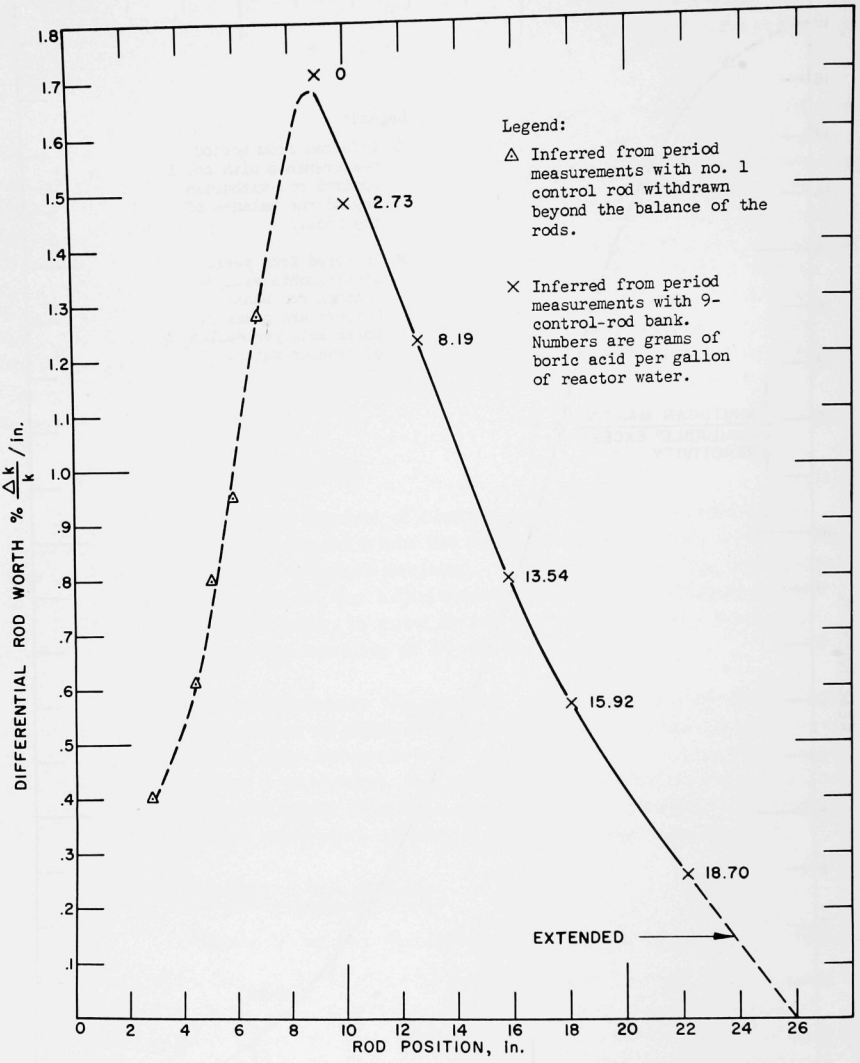

Fig. 12. Differential Reactivity Worth of 9-control-rod Bank vs. Control Rod Position for Core B-1A at 70°F

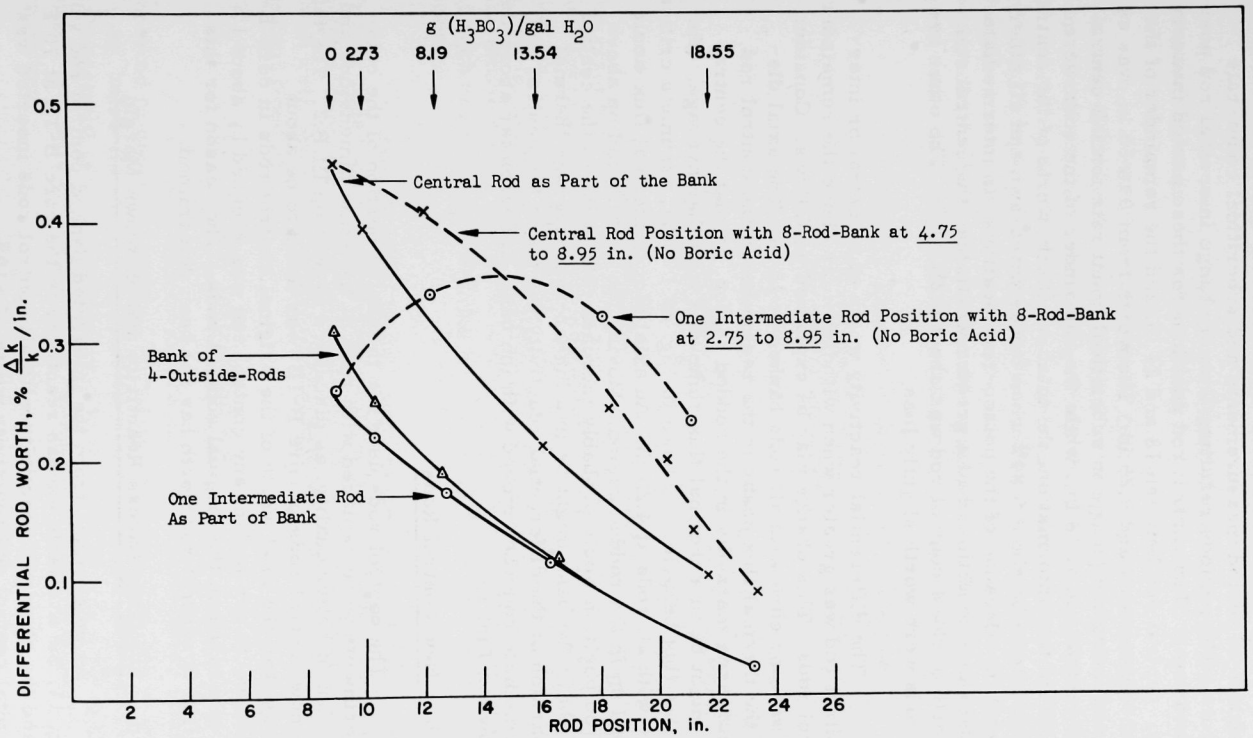

Fig. 13. Differential Reactivity Worth of Control Rods vs. Control Rod Position for Core B-1A at 70°F

The worth of the central control rod alone was estimated by a combination of period measurements and subcritical count-rate measurements. The periods resulting from a change in central rod position were measured. The control rod positions for these period measurements were: central rod between 18 and 24 in. and the remainder of the rods banked between 4.00 and 5.25 in. The worth from 0 to 18 in. was estimated by observing the change in subcritical count rate for the central rod at 0 and central rod at 18 in., while the remainder of the rods were at 4.26 in. From this information, the total reactivity worth of the central rod was estimated to be about 5.84% when it was withdrawn and all other rods were at 0 in. Because of the poison-rod locations, an intermediate rod under the same conditions had a greater worth than the central rod. The total worth of No. 4 control rod was about 6.2% $\Delta k/k$. The other intermediate rods were worth slightly less.

The differential reactivity worth of a central or intermediate control rod was greater when withdrawn far above the remainder of the control rods. This change may be explained as follows: Consider the critical reactor core with all rods banked at 15 in. The axial distribution of the thermal flux peaks in the region below the control rod bank and decreases markedly in the rodded region, so that the central control rod might be in a thermal flux somewhat less than average. (An example of this flux behavior is shown in Fig. 25.) Next, assume a critical reactor core with all rods at 4.26 in. An axial plot of thermal flux would now peak well up in the rodded region. Moving the central rod up above the banked rod position would probably increase this peak, so the central control rod above the bank might be in a higher-than-average thermal flux. Comparison of the differential reactivity worths of the central rod and an intermediate rod when moved with the bank, and when far above the bank, is shown in Fig. 13.

b. New Control Rods

The control rods used for the major portion of the cold critical experiments were replaced with rods of the same dimensions and composition, but of better quality, as discussed in Section III.B.2. The total worth of the new control rods in core B-1B' was found to be about 0.2% $\Delta k/k$ less than the total worth of the original control rods in core B-1B. The reactivity worth per inch of any control rod was reduced by about 1% of the value measured on the original control rods. The reason for this small reduction in control rod worth has not been determined.

c. Available Excess Reactivity and Shutdown Margin

As determined from the integrated banked control rod worth curve in Fig. 11, the available excess reactivity in the core B-1A at 70°F was ~12%, and the shutdown reactivity with all control rods inserted was ~-7%, for a total control rod reactivity worth of ~19%.

3. Void Effects

The reactivity effects of simulated voids in core B-1A were measured at room temperature with boric acid in the reactor water.

Reactivity effects were determined by comparing the critical positions of banked control rods and by period measurements. Banked control rod positions were all greater than 22 in. The average value for the reactivity worth of boric acid solution throughout the core [-0.6% per $g(H_3BO_3)/gal(H_2O)$] was used to correct the void-effect measurements for the effect of displaced boric acid. Any change in the reactivity worth of boric acid due to change in concentration was neglected. Measurements were made with four different configurations, as follows:

a. equally distributed voids in the whole core;

b. voids distributed to simulate a realistic void distribution under low-power conditions;

c. voids concentrated in the center 16 fuel assemblies only (at the reference water-fuel ratio);

d. voids concentrated in the center 16 fuel assemblies only (core with increased water-fuel ratio).

All measurements of the void effect were made by comparing the reactivity effect of void tubes located in coolant channels of the boiling fuel assemblies with water-filled tubes in the same locations, thus cancelling any effect of aluminum. The void tubes, 0.25 in. OD x 0.035 in. wall x $33\frac{5}{8}$ in. long, are sealed 3003 aluminum alloy tubes filled with helium at one atmosphere. The water tubes are the same except for holes drilled at each end to permit flooding with reactor water and/or boric acid solution.

For the experiments with changed water-to-fuel ratio, hollow "water rods" were used to replace fuel rods. A "water rod" has the same outside dimensions as a fuel rod, but the core section is made of 0.038-in.-thick wall, 3003 alloy aluminum tubing with holes drilled at each end to permit flooding.

a. Equally Distributed Voids

For this measurement, 120 void or water tubes were fully inserted in coolant channels. They extended from 8 in. above the core to $1\frac{5}{8}$ in. below the core. The distribution of tubes is shown in Fig. 14. This arrangement gave an average void in the core of only 0.5% of the moderator water, which is equivalent to an estimated 50-100 kw of power at 600-psig conditions.

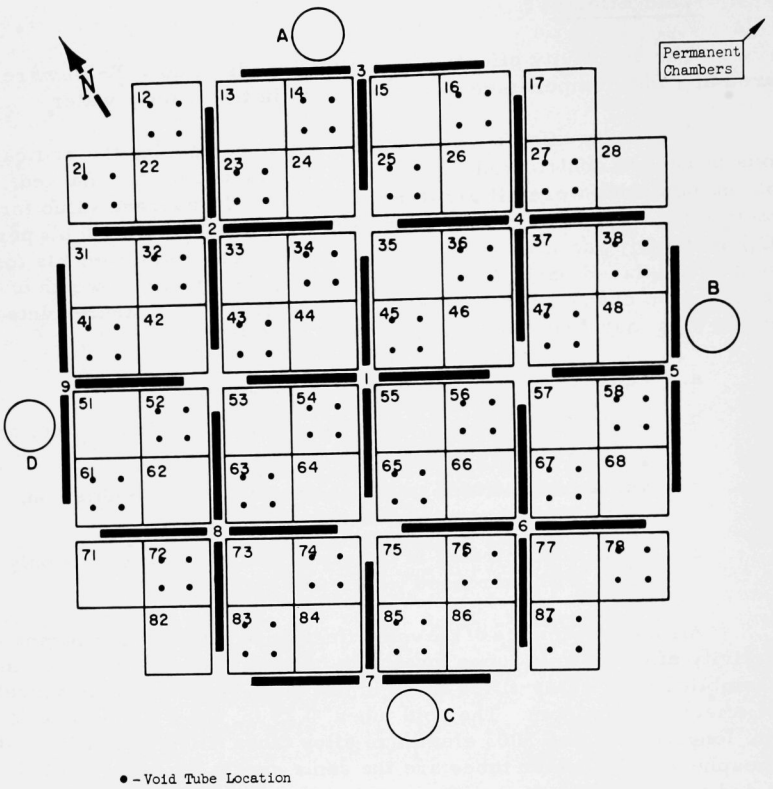

Fig. 14. Uniformly Distributed Void Tube Locations in Core B-1A

When corrected for boric acid displacement, the measured reactivity effect of voids was -0.36% per % void. This value includes some streaming effect due to voids in the upper and lower reflector.

b. Realistically Distributed Voids

To obtain a more realistic idea of the void coefficient in a boiling core, the voids were distributed nonuniformly in zones both axially, radially, and in the upper reflector in an array calculated to simulate an actual void distribution. This arrangement is shown in Fig. 15. Here, again, the total void content of the core only was 0.5% of the moderator, although the total number of void or water tubes used was 264.

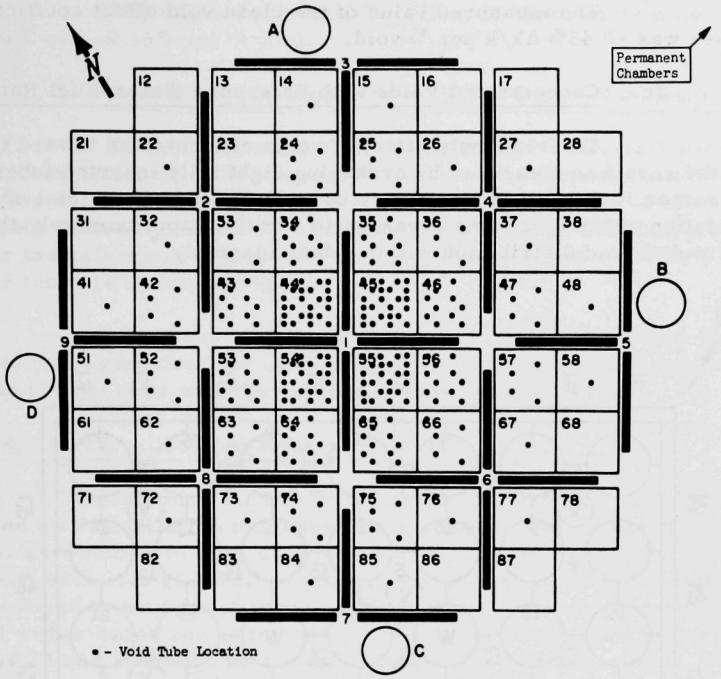

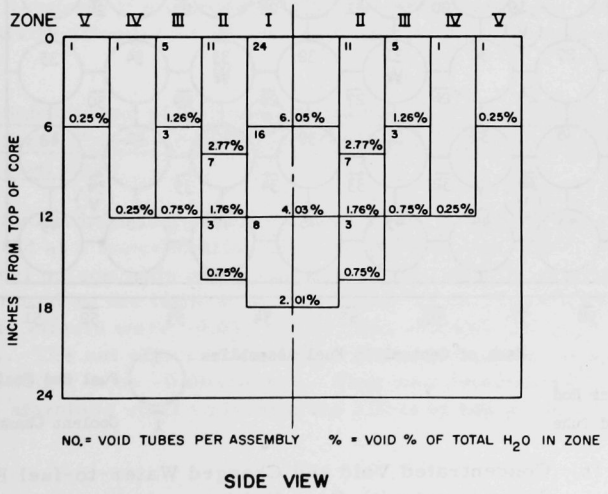

Fig. 15. Realistic Void Distribution Experiment in Core B-1A

The measured value of the clean void effect coefficient for this case was -0.45% $\Delta k/k$ per % void.

c. Concentrated Voids with Reference Water-Fuel Ratio

The reactivity effect of voids concentrated toward the center of the core was measured by arranging eight fully inserted tubes in each of the center 16 assemblies only, as shown in Fig. 16, for a total of 128 tubes. The location of the tubes was arranged to simulate approximately the expected radial void distribution within a fuel assembly.

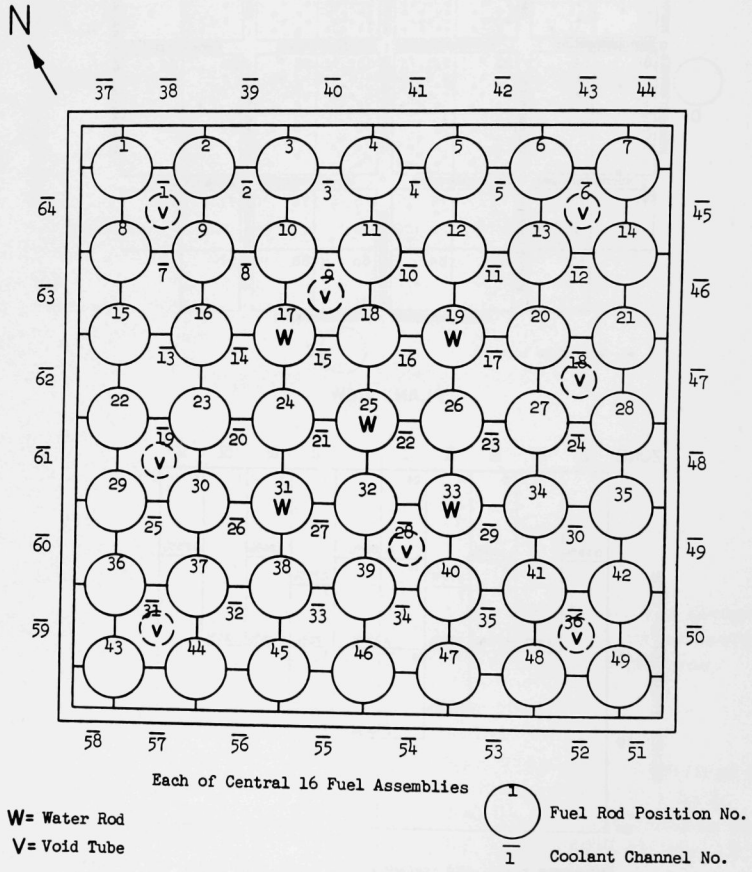

Fig. 16. Concentrated Void and Changed Water-to-fuel Ratio Experiment with Core B-1A

The measured reactivity effect of clean voids under these conditions was -0.55% per % void.

d. Concentrated Voids with a Higher Water-Fuel Ratio

To determine the effect of increased water-fuel ratio on the reactivity effect of voids, five fuel rods in each of the central 16 fuel assemblies only, located as shown in Fig. 16, were replaced with water rods. This raised the $H_2O:UO_2$ volume ratio in these assemblies from 2.21, for the reference core B-1A, to 2.51. The distribution of void tubes or water tubes is shown in Fig. 16.

The measured clean void effect for the increased water-fuel ratio was approximately -0.27% $\Delta k/k$ per % void, or about one-half the value for the core with the reference water-to-fuel ratio.

4. Removal of Fuel Rods or Fuel Assembly

To determine the reactivity effect of removing fuel rods, a water rod was installed in the place of a fuel rod in the center of the four fuel assemblies in core positions 33, 34, 43, and 44 (see Fig. 9) in core B-1A with 18.6 $g(H_3BO_3)$ per gallon of reactor water. This substitution was found to have an effect of -0.0026% $\Delta k/k$ per rod. Replacing a fuel rod with a water rod in the center of the fuel assemblies in core positions 23 and 24 produced a slightly negative reactivity effect. These values are not corrected for boric acid displacement.

Removal of a complete fuel assembly from core position 45 gave a reactivity effect of -2.7% as measured in the core without boric acid.

5. Substitution of Boron-Stainless Steel Poison Rods, Stainless Steel Poison Rods, Water Rods, and 9.90-w/o Enriched Fuel Rods

Substitution experiments were made in core B-1A poisoned with boric acid at a concentration of 18.64 $g(H_3BO_3)/gal(H_2O)$. Boron-stainless steel poison rods were substituted for the fuel rods in three positions denoted by the letters "a," "b," and "c" in Fig. 9. The resulting reactivity effects were -0.09, -0.093, and -0.049% per poison rod, respectively. The net effect of the boron alone in one poison rod in position "a" was found to be -0.064% $\Delta k/k$. This was determined by comparing the effect of stainless steel rods with the effect of boron-stainless steel rods.

The reactivity effect of replacing two fuel rods with poison rods in the positions marked "f" in Fig. 9 to increase the number of poison rods from 32 to 34, in the core at room temperature with no boric acid, was measured to be -0.14% per poison rod.

Substitution of water rods for fuel rods in the "a" position made a very slight negative change. Substitution of five water rods for fuel rods in each of the center 16 assemblies in the locations shown in Fig. 9 produced a reactivity effect of -0.45%.

Substituting single 9.90-w/o enriched for 4.95-w/o enriched fuel rods in the isolated positions marked "a," "d," and "e" in Fig. 9 resulted in reactivity changes of +0.011, +0.012, and +0.003% per rod, respectively.

6. Boric Acid Effects

The addition of boric acid for control rod calibration gave an essentially linear reactivity effect at lower concentrations. Figure 17 indicates banked-control-rod critical positions vs. the boric acid concentration in core B-1A. When correction was made for the variation in control rod worth, the average reactivity effect of boric acid was found to be -0.6% per $g(H_3BO_3)/gal(H_2O)$.

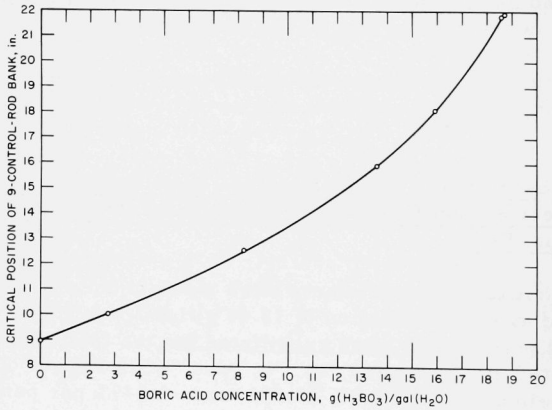

Fig. 17. Critical Position of 9-control-rod Bank vs. Boric Acid Concentration for Core B-1A at 70°F

D. Neutron-flux Mapping

Core physics calculations during the design of BORAX-V produced smooth flux plots for an ideal homogeneous boiling core.(1) Since the core of BORAX-V is not homogeneous, it was desirable to determine the local axial and radial variations in flux within a fuel assembly and from assembly to assembly, primarily in order to provide information on the power distribution within the core for the heat-engineering analysis. The calculated flux distributions in the core provided a gross peak-to-average power ratio. Calculations of the effect of water and control rod channels between assemblies provided a local peak-to-average power ratio within a fuel assembly, but these numbers needed to be verified. In addition, since the thermal-hydraulic analysis of the natural-circulation system was based on summing the flows through the individual assemblies, and since the flows and exit qualities of the assemblies were dependent on the power produced within the individual assemblies, a method of obtaining the "assembly-to-average" power ratio for the various core positions was required. Still another reason for extensive measurement of flux distributions in the boiling core was to check the validity of the calculational techniques.

1. Distributions of Coarse Neutron Flux

The measurement techniques and counting equipment used for both coarse- and fine-flux mapping are described in this section. After axial measurements in a number of radial positions were taken with control rods nearly withdrawn from the core, an experimental study was made of the neutron-flux distribution adjacent to a partially inserted control rod. Experiments were also run to determine the level of neutron flux at the reactor vessel shell and the effect on neutron-flux distribution of boric acid concentration in the reactor water.

a. Measurement Techniques and Counting Equipment

Three different detector materials were used in the flux-mapping experiments:

(1) gold wire (of 0.032-in. diameter);

(2) uranium-zirconium wire, 3.379 w/o U, 93.13-w/o enriched (of 0.031-in. diameter);

(3) uranium-aluminum wire, 7.78 w/o U, 93.1-w/o enriched (of 0.032-in. diameter).

Comparable irradiations were made with short segments and continuous wires of both gold and the uranium alloys at various radial points. The segments were $\frac{3}{8}$ in. long and arranged within a wire holder so that their longitudinal centers were at 1-in. intervals, beginning at the base of the fuel and rising vertically to 5 in. above it. Aluminum spacers were placed between wire segments. The continuous wires were placed in the same type of holder. The flux-wire holders were made of either stainless steel or aluminum tubing, 0.125 in. dia x 0.020 in. wall, with a support and guides for reproducible positioning.

Both aluminum and stainless steel wire holders and a representative wire segment loading are shown in Fig. 18. The wire holders were inserted into a water channel of the fuel assembly, and were positioned by the upper and lower grids. The upper shoulder of the holder controlled the insertion distance by resting on the upper grid of the fuel assembly, as shown in Fig. 19. Water-channel and fuel-rod locations for a boiling fuel assembly are shown in Fig. 16. To normalize counts, a monitor wire of each material used was irradiated at the same radial and axial position in each irradiation for purposes of comparison.

Counting of the activity induced in the wire segments was accomplished with scintillation crystals of 1.0-mm-thick anthracene for betas and sodium iodide for gammas. Both types of counting were done on some of the early irradiations, but since the gamma counting offered more favorable statistics and better discrimination control, the activity of the segments was gamma-counted in a standard pig arrangement. Preset count control using the monitor foil of the material being counted allowed automatic decay correction. An overall view of the counting equipment is shown in Fig. 20.

A rotary scanner was used for counting the continuous wires. The wires were attached to the rim of a large aluminum disk with a lead hub and passed in front of the counting head by an automatic sequencing system which controlled the incremental movement of the wheel, counting time, and data printout. A portion of the system allowed regulation of the counting time per interval by the same preset count technique used for the segments. Because of collimation and shielding problems, gamma-counting of the continuous wires was not successful. Therefore, the continuous wires were counted with the beta crystal detectors. The beta-counting results were discontinuous, but the flux shapes obtained compared well with those inferred from gamma counting of wire segments.

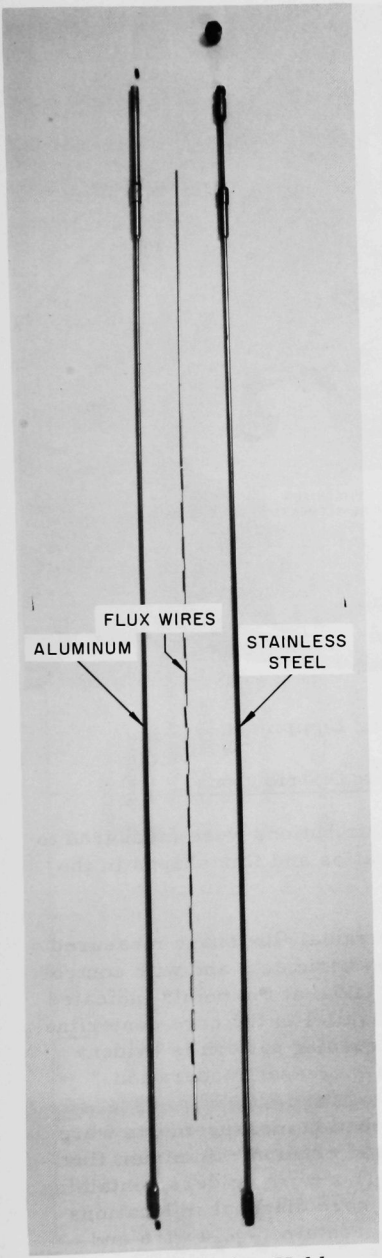

Fig. 18. Flux-wire Holders

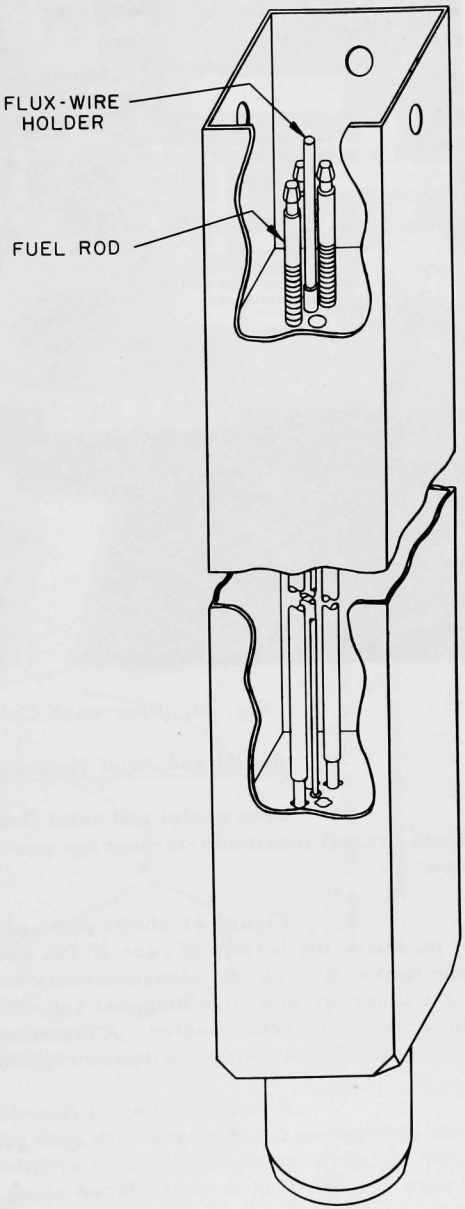

Fig. 19. Flux-wire Holder in Fuel Assembly

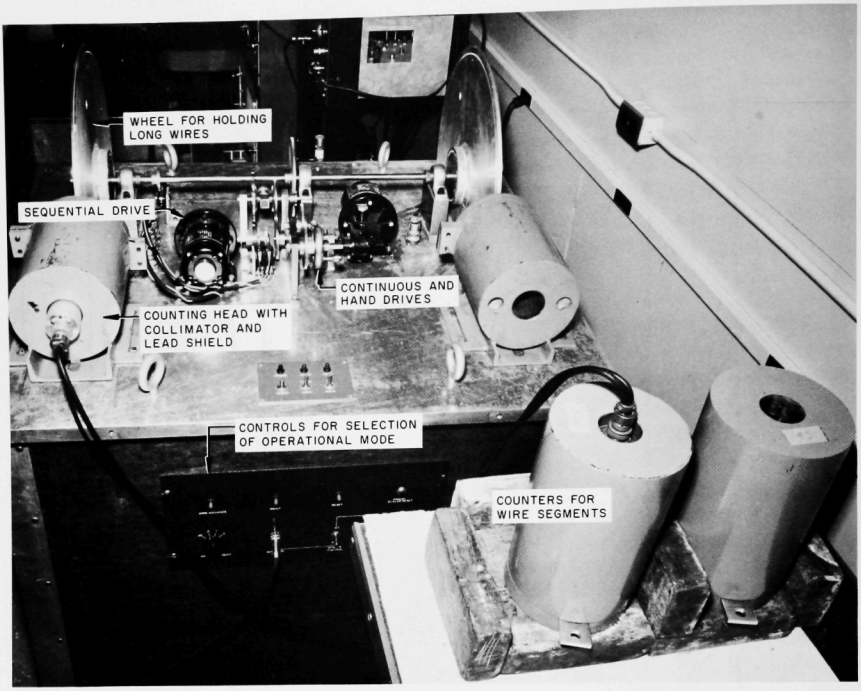

Fig. 20. Flux-wire Counting Equipment

b. Radial and Axial Neutron-flux Distributions

Both radial and axial flux distributions were measured to obtain overall maximum-to-average power ratios and flux shapes in the core.

Figure 21 shows plots of the radial flux shape measured $3\frac{1}{2}$ in. above the bottom of core B-1B, with no boric acid and with control rods banked at 8.68 in. Measurements were taken at the points indicated in the diagram on a core diagonal and also parallel to the core centerline. The wires were beta-counted. A significant cusping pattern is evident within each fuel assembly between regions of increased moderation.

A number of axial flux-distribution measurements were made during two irradiations with both gold and uranium-aluminum flux wires. In each irradiation, twelve aluminum flux-wire holders containing 30 wire segments each were placed along the core diagonal in locations shown on the diagram in Fig. 22. Six holders contained gold wire and

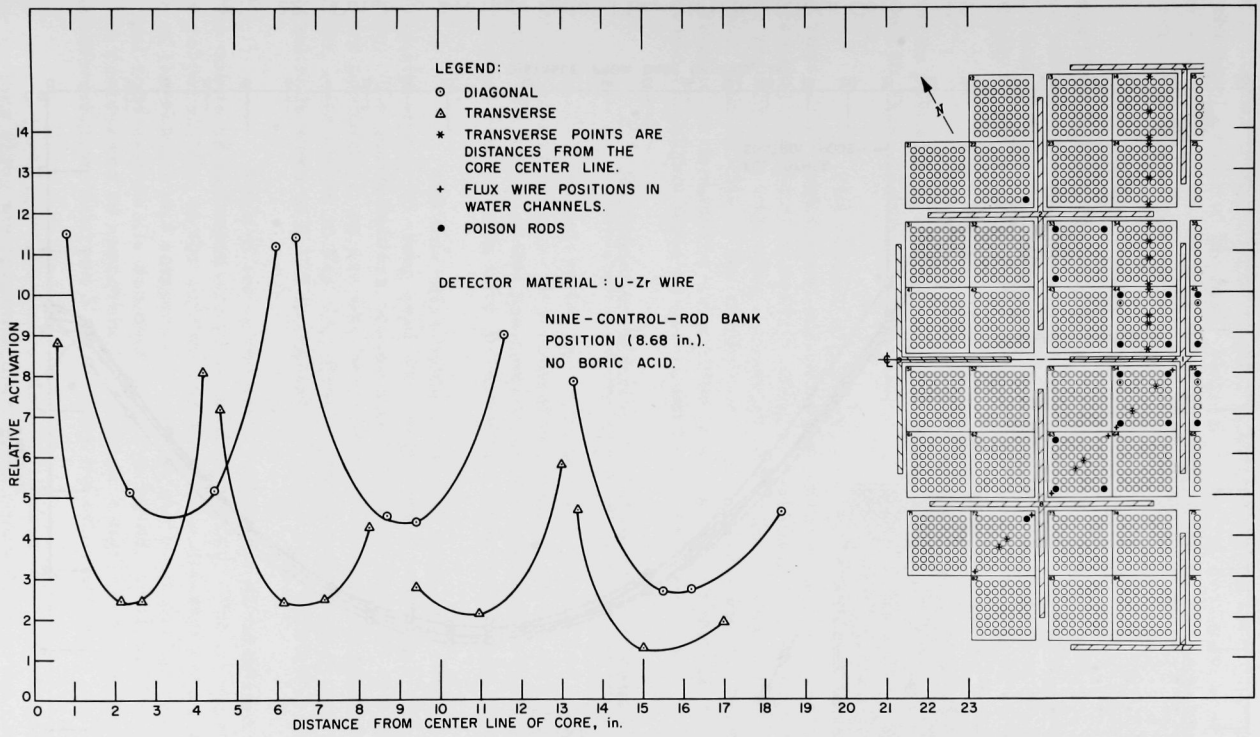

Fig. 21. Radial Flux Plots at $3\frac{1}{2}$ in. from Bottom of Core B-1B

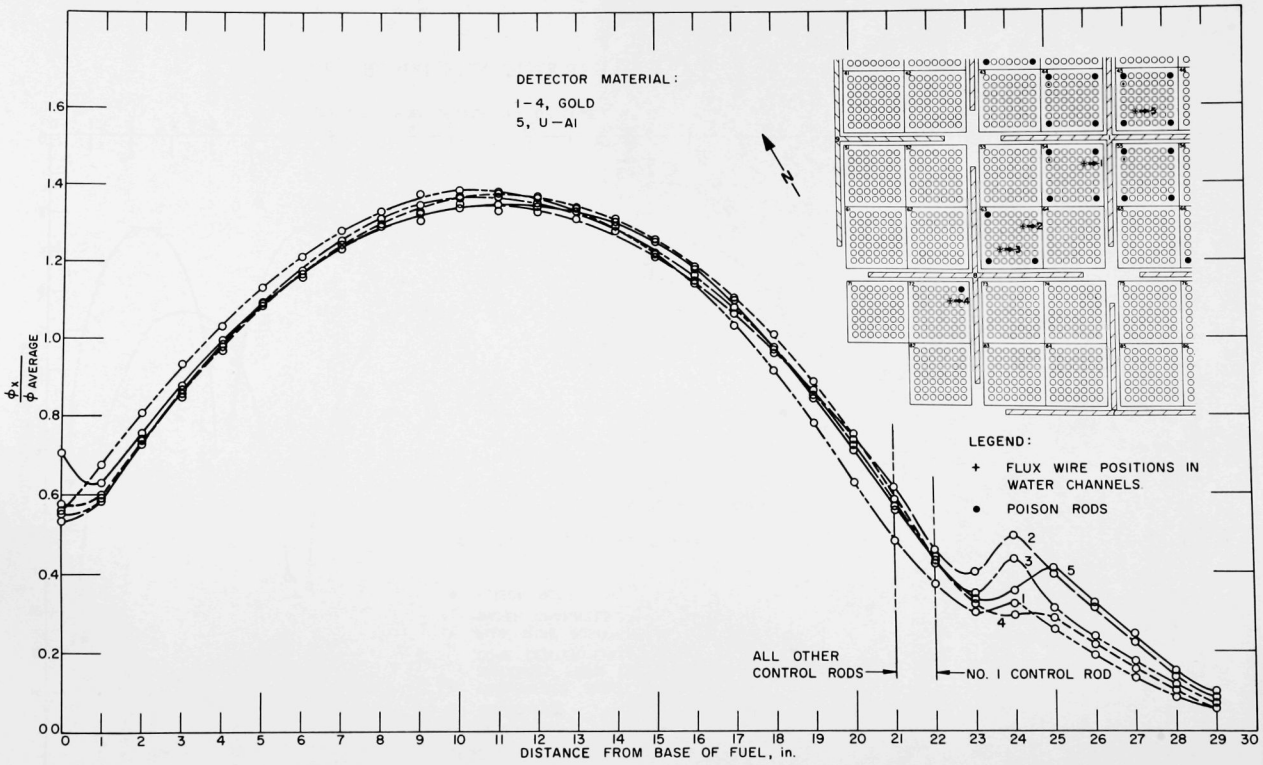

Fig. 22. Point-to-average Axial Flux Distribution in Core B-1C

six contained U-Al. Single monitor foils of gold and of U-Al were located at the axial center of the fuel. Four of the radial positions used in the first run were rerun with the alternate detector material to obtain checks of point symmetry between quadrants of the core.

Figure 22 shows five axial plots measured at various points along the diagonal of core B-1C. The results were normalized by plotting on a point-to-average basis. A comparison of measurements taken with gold and U-Al may be made from curves 1 and 5, which were taken at radially symmetric points.

Additional axial plots on a relative count basis taken at various positions in core B-1C, both on and off the core diagonal, are shown in Figs. 23 and 24.

The results of point-symmetry checks between quadrants and runs of the experiment indicated that, within the error limits of the determinations, point symmetry along the diagonal axis was good. Further assumptions regarding symmetry cannot be made from the data collected. The results of the continuous-wire counting are not presented, but no significant departures were noted from the axial shape of the flux at specific radial positions as determined with the segments.

c. Neutron-flux Distribution Adjacent to a Control Rod

To determine the influence of a control rod with an aluminum control rod follower in a control rod channel on the axial flux distribution at various radial positions in an adjacent fuel assembly, an irradiation was made in core B-1C with no boric acid in the reactor water.

The flux-wire holders were of aluminum, and each contained eighteen $\frac{3}{8}$-in.-long gold-wire segments traversing 17 in. of the fuel region. The seven holders occupied seven water channels of a fuel assembly in core position 43, on one line perpendicular to the west blade of control rod No. 1, as shown in Fig. 25. Reactor water temperature was 71°F. All control rods were at 8.778 in. except the No. 1 rod, which was at 8.842 in.

Four of the seven axial count-rate distributions for four of the points as indicated are presented in Fig. 25. The points lie along a line perpendicular to the control rod at various distances from it. Inspection of the results and comparison with the distributions obtained with the control rods essentially removed show the effect on the axial distribution as the control rod is approached. There is a significant depression in the axial distributions (curves 3 and 4) near the control rod.

Figure 26 shows plots of transverse relative count-rate distributions along the perpendicular to the control rod in the control rod region and below it. The plots represent one axial point in the seven transverse positions measured. The shape of the distribution below the

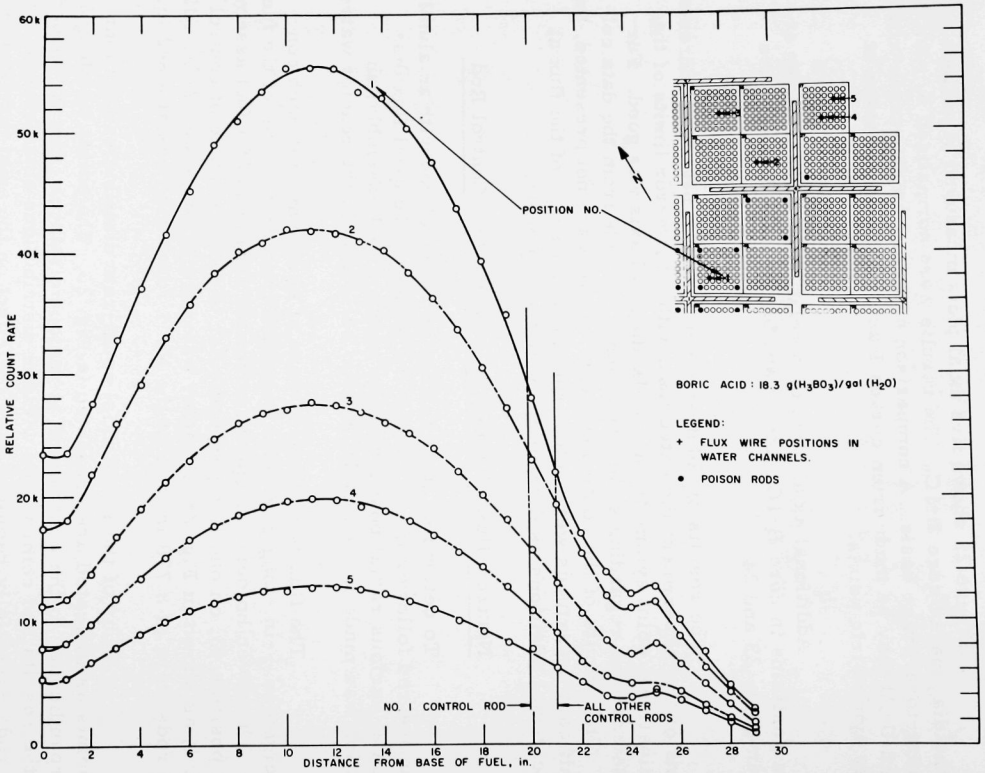

Fig. 23. Axial Flux Distributions (Gold Detectors) in Core B-1C

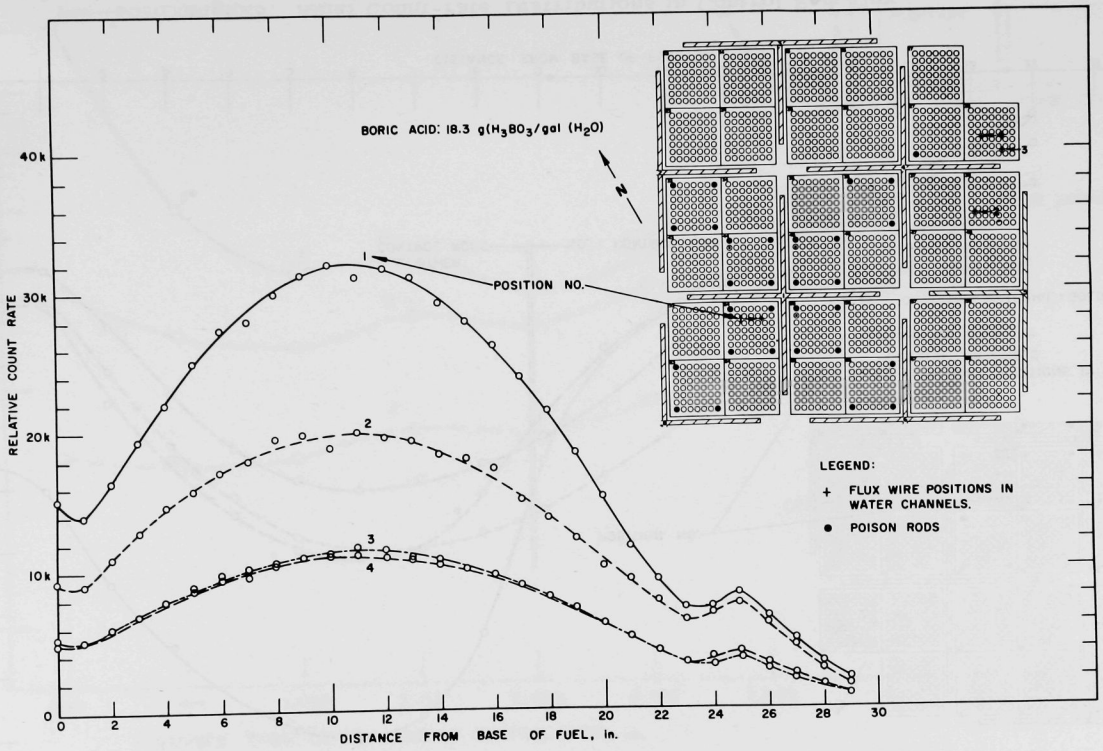

Fig. 24. Axial Flux Distributions (U-Al Detectors) in Core B-1C

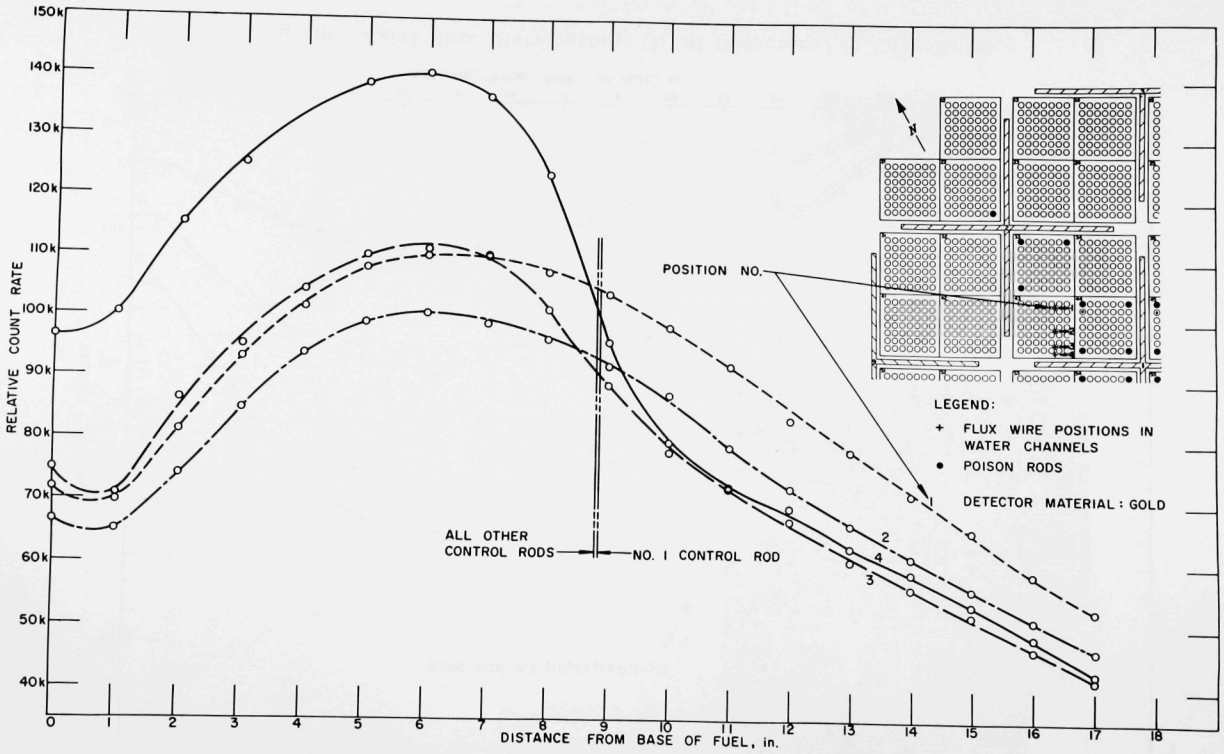

Fig. 25. Axial Count-rate Distributions in Control Rod Flux Depression Study with Core B-1C

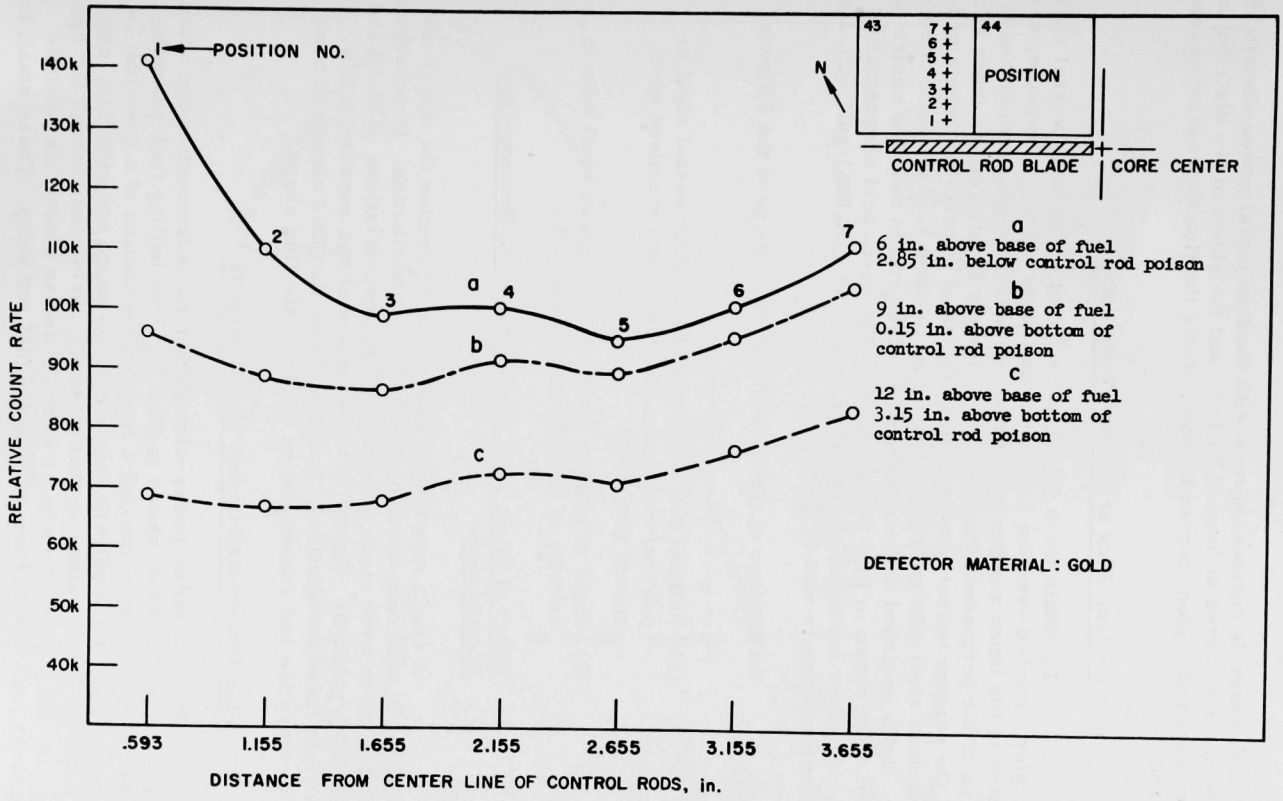

Fig. 26. Transverse Plots for Control Rod Flux Depression Study with Core B-1C

control rod, shown in curve a, agrees with the fine radial power-distribution measurements reported in Section III.D.2.; and the shape of the distribution in the control rod region, curves b and c, shows the flux depression caused by the rod.

d. Neutron Flux at Reactor Vessel Shell

To obtain the level of activation at the reactor vessel shell, bare, highly enriched uranium foils, enclosed in an aluminum capsule, were irradiated at the inner surface of the reactor vessel. To determine the attenuation of the permanent stainless steel thimble located on the inner surface of the reactor vessel, another foil in the same capsule was contained in a stainless steel tube with a 0.035-in. wall thickness. As a point of reference, highly enriched uranium foils were also located near the center of core B-1A, as shown in Fig. 37 (see p. 57). The boric acid concentration in the reactor water during this irradiation was 18.68 $g(H_3BO_3)/gal(H_2O)$, and the water temperature was 76°F.

An average of three counts of the foils gave the following results:

(1) Ratio of foil activity at the reactor vessel shell to point-of-reference in the core (no stainless steel cover) was 0.009.

(2) Ratio of activity of foil in a stainless steel tube to activity of unenclosed foil was 0.97.

e. Effect of Boric Acid Concentration on Neutron-flux Distribution

A single experiment was run to determine the effect of a change of boric acid concentration on axial flux distribution. Irradiations of gold flux wires were made in core B-1C at concentrations of 16.55 and 18.3 $g(H_3BO_3)/gal(H_2O)$. Figure 27 shows a plot of two representative curves from these irradiations. It is concluded that this change in boric acid concentration had essentially no effect on the flux shape.

2. Fine Power-distribution Measurements

The fine radial power-distribution measurements were obtained by means of the equipment shown in Fig. 28. Two boiling fuel-assembly boxes were modified by removing a replaceable section of a box side. A $3\frac{3}{4}$-in.-sq x $\frac{1}{2}$-in.-thick polyethylene block was prepared with forty-nine $\frac{3}{8}$-in. holes on $\frac{1}{2}$-in. centers so that fuel rods could pass through the block. Two $\frac{1}{32}$-in.-dia x $\frac{1}{4}$-in.-deep holes were drilled as closely as possible (about 10-15 mils apart) from each of the fuel rod holes. These small holes

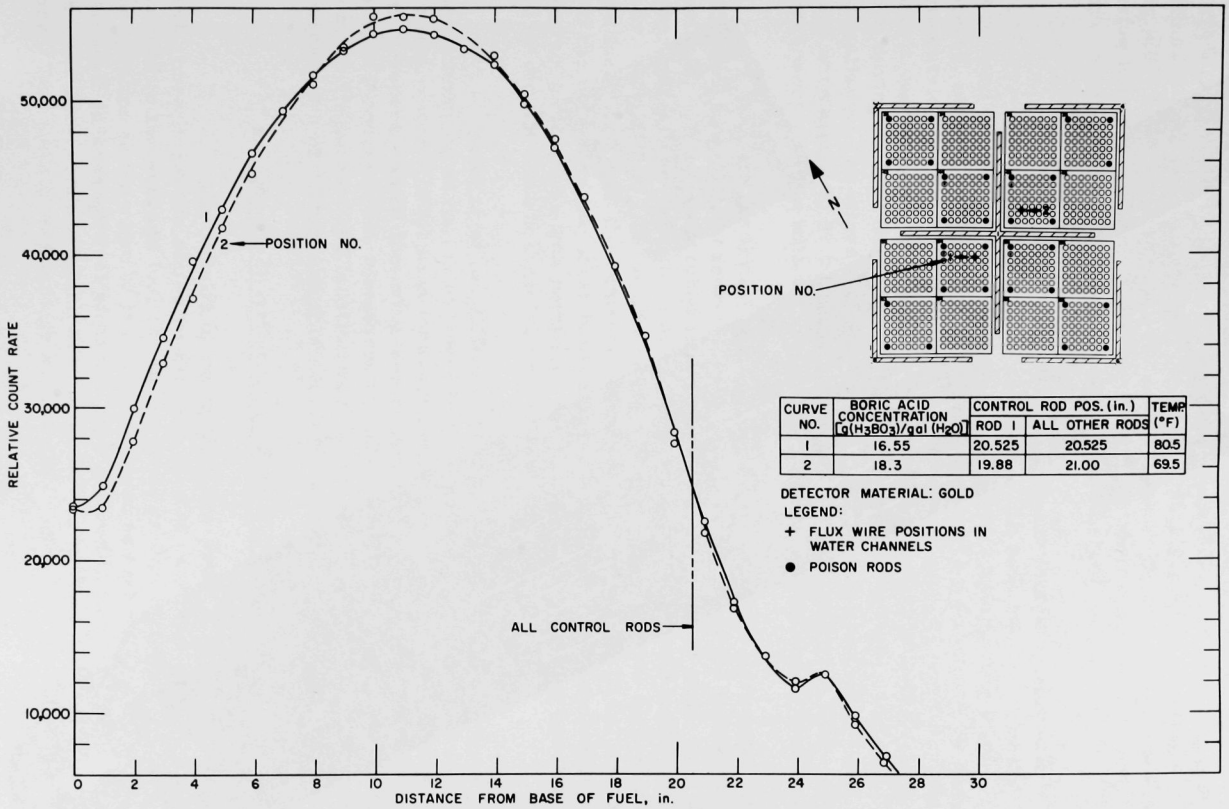

Fig. 27. Axial Flux Distribution for Boric Acid Check in Core B-1C

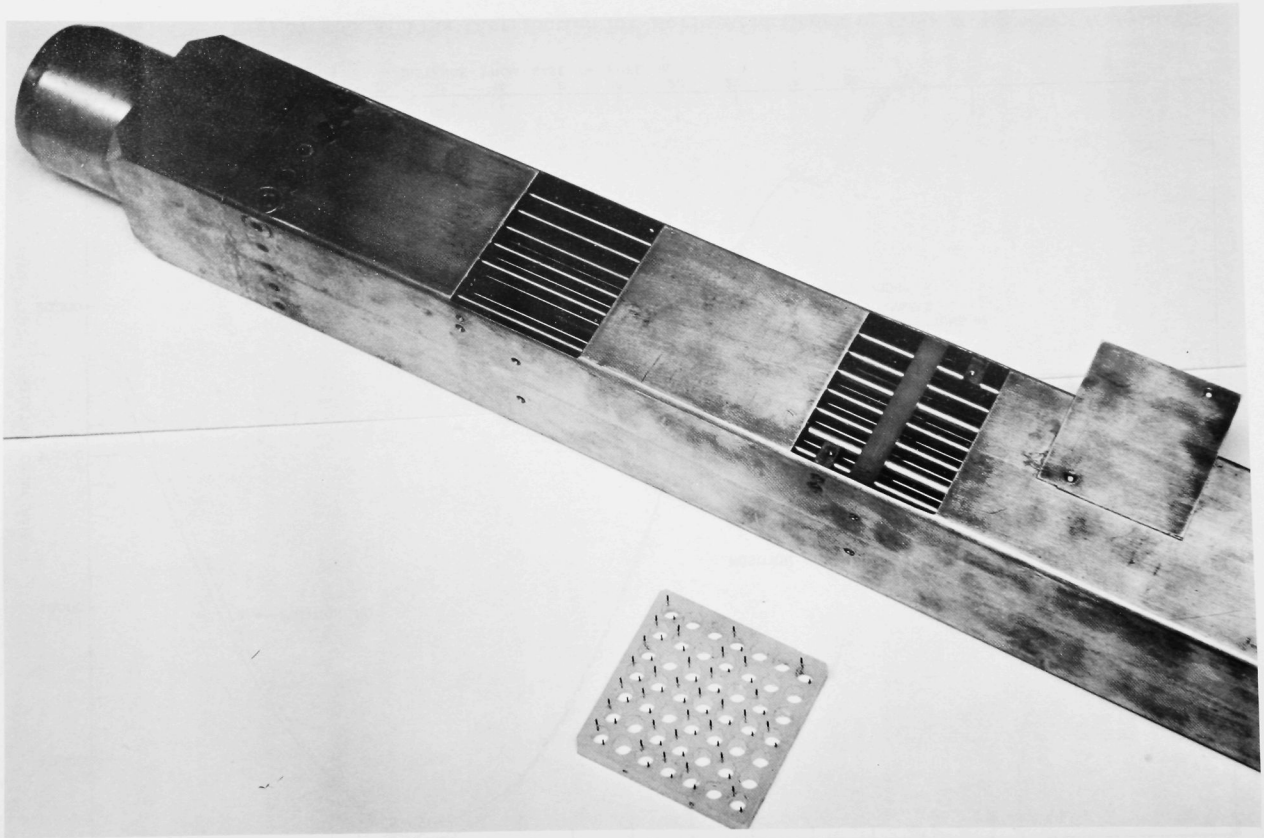

Fig. 28. Fuel Assembly with Flux-wire Tray

were used to position and hold securely $\frac{3}{8}$-in.-long x 0.031-in.-dia Zr-3.379% U (93% U^{235}) wires. Each polyethylene flux-wire tray was loaded with 62 flux wires, two each adjacent to 31 fuel rod holes, as shown in Fig. 28. The flux-wire trays were positioned near the midplane of the active length of the core to provide two axial locations, one for use with boric acid in the reactor water and one for use with no boric acid.

After the wires were loaded into the flux-wire trays, the trays were inserted into a fuel assembly. Two such fuel assemblies were used during each irradiation, and flux-wire assemblies were located, in turn, in each of the nine core positions which make up the symmetrical portion of an octant of the core. A monitor wire was placed in an aluminum flux-wire holder in a uniform location elsewhere in the core during each of the irradiations, so that the data from each could be normalized. The wires were nearly uniform in length and weight, but were normalized to 31.0 mg for the purpose of analyzing the data. All wires were counted with the counting equipment described in Section III.D.1.

After the initial mapping of one octant of the core was completed, additional fine-flux measurements were made to determine the effect of replacing 4.95-w/o enriched fuel rods with other types of rods, such as water rods, boron-stainless steel poison rods, or 9.90-w/o enriched fuel rods. In addition: (1) the flux shape adjacent to the central control rod was measured with the central control rod inserted about 10 in. farther into the core than the other banked rods; and (2) the flux distribution across two fuel assemblies was compared for the cases in which the reactor water did or did not contain dissolved boric acid.

Because of the difficulty of drawing meaningful curves due to the pronounced variation of power across a fuel assembly, the data for the fine power-distribution measurements are presented in terms of relative numbers. Each flux wire was counted for an interval corresponding to 10,000 counts of the monitor wire. The counts on the two wires adjacent to a particular fuel rod location were averaged after being normalized to a wire mass of 31 mg, and this average was assigned to that fuel rod.

a. Power Distribution in Core B-1B

The results of the initial, fine power mapping of one octant of the core B-1A are shown in Fig. 29. In this case, all the data were normalized to the average fuel rod in the core, so that the number of each fuel rod location is the ratio of the local-to-average fuel rod power production. The peak-to-average fuel power, 1.99, occurred in fuel assembly position 36. The fuel rod locations which are blacked out contained boron-stainless steel rods. Two additional numbers appear above each fuel assembly in Fig. 29.

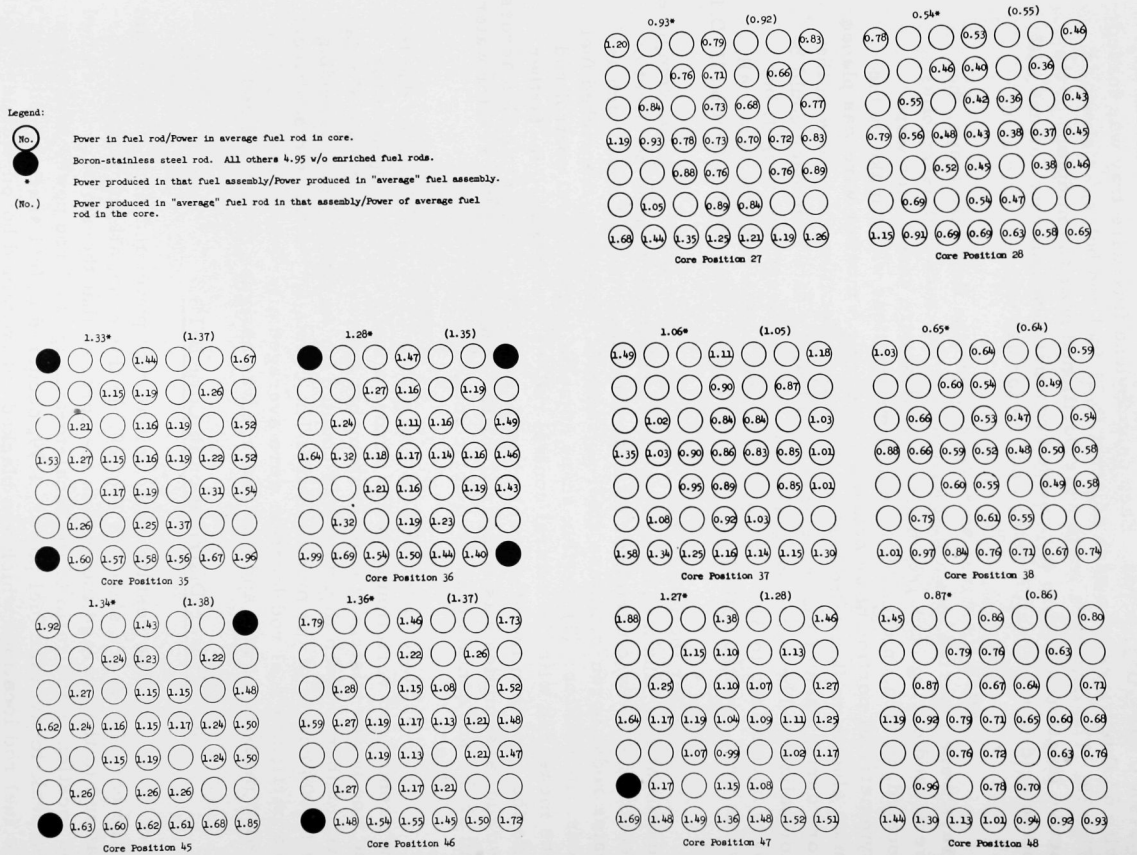

Fig. 29. Fine Power-Distribution in Core B-1A

The first is the ratio of the power produced in the fuel assembly to the power in an "average" fuel assembly in the core. The second number (in parentheses) is the ratio of the power produced by the "average" fuel rod in the fuel assembly to the power produced by the average fuel rod in the core. The two numbers differ because the number of fuel rods in the various assemblies differed.

The data indicated that the degree of symmetry around a diagonal through the core center was not uniform. In general, however, the values of power for corresponding points agreed within 2 to 3%.

The average value of the single-fuel-rod power within a fuel assembly was computed in the following manner:

(1) The values for the four corner fuel rods were added.

(2) The values for fuel rod locations 4, 22, 28, and 46 (see Fig. 16 for explanation of fuel rod locations) were added and multiplied by 20. This took into account the peripheral rods other than the corners.

(3) The values for fuel rods in locations 11, 23, 27, and 39 were added and multiplied by 4. This took into account all the rods just inside the periphery.

(4) The values for fuel rods in locations 18, 24, 26, and 32 were added and multiplied by 2.25. This took into account the nine central fuel rods.

(5) The results in (1), (2), (3), and (4) were added and divided by 49, the number of fuel rods per fuel assembly.

In computing the average relative power of a fuel rod in an assembly, the above procedure was modified so only fuel rods, and not poison rods, were counted.

The average value of the power for an assembly was determined by taking the sum in (5) above, multiplying it by 4 or 8, depending on the number of corresponding assemblies in the core, obtaining a grand total of the results for all the fuel assemblies, and dividing this grand total by 60.

To flatten power distribution, the data of Fig. 29 were used, together with experiments regarding the single-control-rod criticality criterion, to determine the number and location of the boron-stainless steel poison rods for the core loading B-1B shown in Fig. 10. The effect of boron-stainless steel poison rods is quite localized so far as flux shaping is concerned, and even the flux in an adjoining fuel rod is hardly affected by replacing a fuel rod with a poison rod. Consequently, Fig. 29 can be

considered a valid picture of the fine-flux distribution in core B-1B at room temperature if the proper placement of poison rods is superimposed on Fig. 29. This has been done, and the results for core B-1B are shown in Fig. 30.

b. Power Distribution with Water Rods and 9.90-w/o Enriched Fuel Rods near Core Center

After the first mapping of an octant of the core was completed, the effect of varying the composition of a center fuel assembly in core B-1A was investigated. In addition to the configuration shown for core position 45 in Fig. 29, two other loadings in corresponding core positions were used. The second loading contained eight 9.90-w/o enriched fuel rods surrounding a water rod in the center of the assembly, while the third contained four water rods on the diagonals adjacent to the center rod. Layouts of the 3-assembly configuration are shown in Fig. 31. In this figure, the ratio of the power produced in a given fuel rod to the power produced in an average rod in that fuel assembly is shown. The assembly with four poison rods in the corners and four water rods near the center had the lowest peak-to-average value, namely, 1.12. In the assembly with the 9.90-w/o enriched rods, the peak value occurred at one of the 9.90-w/o rods. The 9.90-w/o rods had the same type of flux wires adjacent to them as the 4.95-w/o enriched rods, and the assumption was made that exactly twice as much power was produced in a 9.90-w/o rod as in a 4.95-w/o rod with the same number of counts on its flux wires.

The two right-hand assemblies in Fig. 31 (b and c) were irradiated at the same time, so that their power levels are consistent with each other. The data for the reference fuel assembly (see Fig. 31a) were obtained earlier. These data indicate that the position of the monitor wire in the two cases (Fig. 31b and c) was not the same, since 36% more power was generated in the 9.90-w/o rod assembly than in the reference assembly, which appears to be too great an increase. The local-to-average values are not affected by the inconsistency of the monitor wire, however. The raw data indicated that the 9.90-w/o rod assembly produced only 9% more power than the water rod assembly, even though it contained 46 fuel rods (eight of them 9.90-w/o enriched) and the water rod assembly contained only 41 fuel rods, all 4.95-w/o enriched. The water rod assembly appears to be the more desirable configuration, since its flatter power distribution will allow 13% more power to be produced in an assembly of this composition than in the 9.90-w/o rod assembly for a given peak fuel rod power.

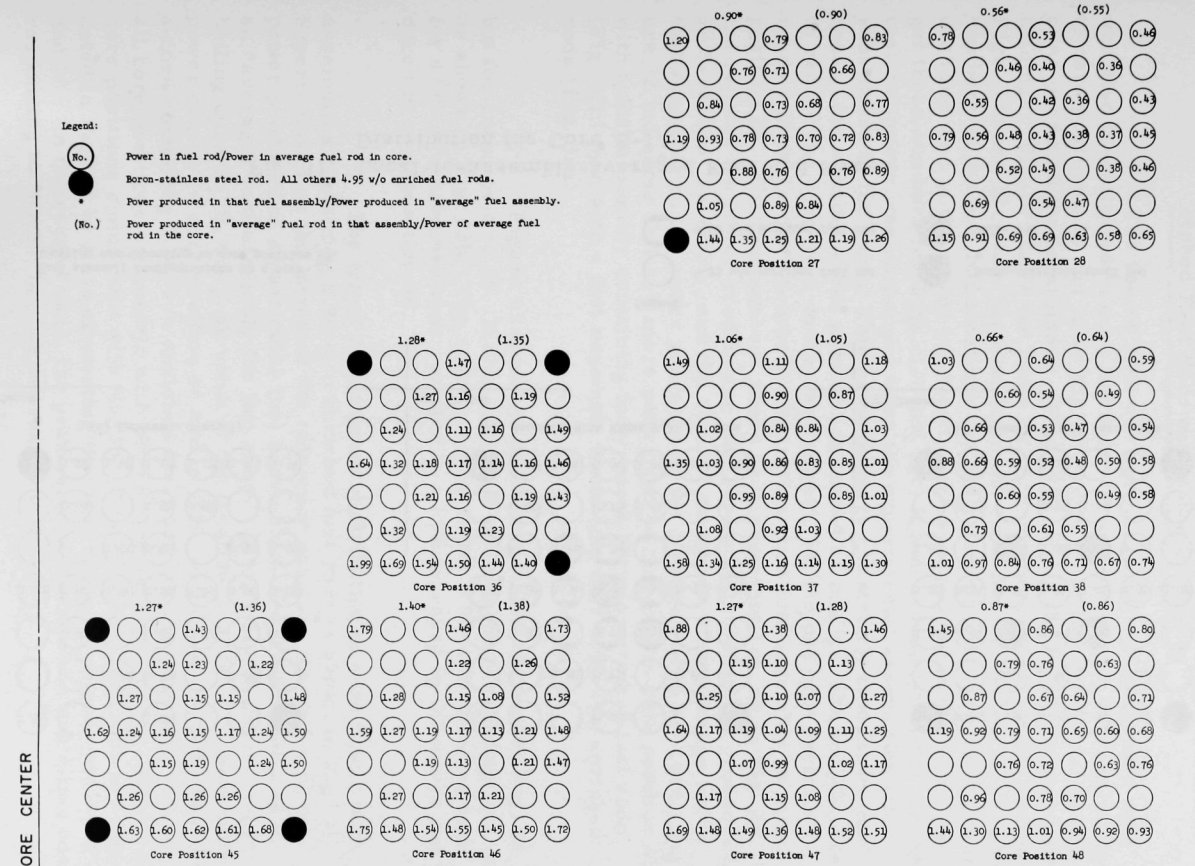

Fig. 30. Fine Power Distribution in Core B-1B

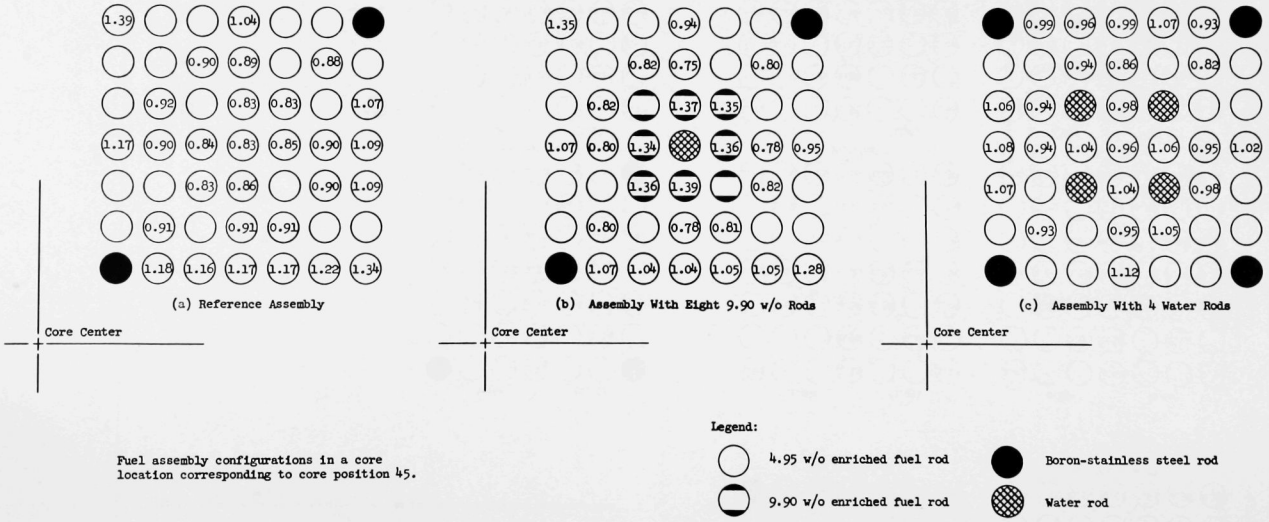

Fuel assembly configurations in a core location corresponding to core position 45.

Fig. 31. Local-to-assembly-averaged Fuel Rod Power Distribution for Core B-1A

c. Power Distribution with Water Rods and 9.90-w/o Enriched Fuel Rods near Core Periphery

The use of 9.90-w/o enriched fuel rods and water rods was also investigated in core B-1B for the core positions corresponding to core positions 28 and 38 in Fig. 29, since these two peripheral assemblies produced the least power. Figure 32 shows the results of the varied loadings. Figure 32a is the same as core position 28 in Fig. 29, whereas Figs. 32b and 32c show the data from the experiments in core B-1B. The numbers in the fuel rod locations are the ratios of the power produced in each fuel rod to the power produced in the average rod in the core. To get these numbers for Figs. 32b and 32c, it was assumed that the average fuel rod power was unchanged when the experimental assemblies were substituted in the core. This assumption is not strictly true (since one reason for wanting to use assemblies loaded as in Figs. 32b and 32c was to reduce the core peak-to-average power), but the use of it permits a ready comparison of various configurations in a fuel assembly in core position 28. The two numbers above each assembly are, as in Fig. 29, the ratio of the power produced in that assembly to the power produced in an "average" assembly, and the ratio of the power of an average rod in that assembly to the power produced in the average rod in the core. Figure 32 indicates that 35% more power can be obtained in core position 26 with a fuel assembly containing forty-one 9.90-w/o enriched fuel rods (Fig. 32c) than with a fuel assembly containing only 4.95-w/o enriched rods (Fig. 32a).

Figure 33 presents data comparable to those in Fig. 32, but for core position 38. In this case only one alternative loading was used, as shown in Fig. 33b. The substitution of thirty 9.90-w/o enriched rods for 4/95-w/o enriched rods resulted in a 69% increase in the power produced in core position 38.

The effect on the gross distribution of core power with assemblies containing 9.90-w/o enriched fuel rods is shown in Fig. 34. Superimposed on the layout of the reference core are the ratios of the power produced in a particular fuel assembly to the power produced in an "average" fuel assembly for two cases. In the case of the reference boiling core B-1B, the peak value of the local-to-average fuel-assembly power occurs in core position 46 and is 1.40. A second case was based on a core containing 9.90-w/o enriched fuel rods, as shown in Fig. 32c, in all core positions symmetric with No. 28, and as shown in Fig. 32b for all core positions symmetric with No. 38. (The 9.90-w/o fuel rods are indicated in Fig. 34 by lines connecting the 9.90-w/o rods in core positions 68 and 78.) In the second case, the peak value still occurs in a position corresponding to No. 46, but has decreased to 1.29.

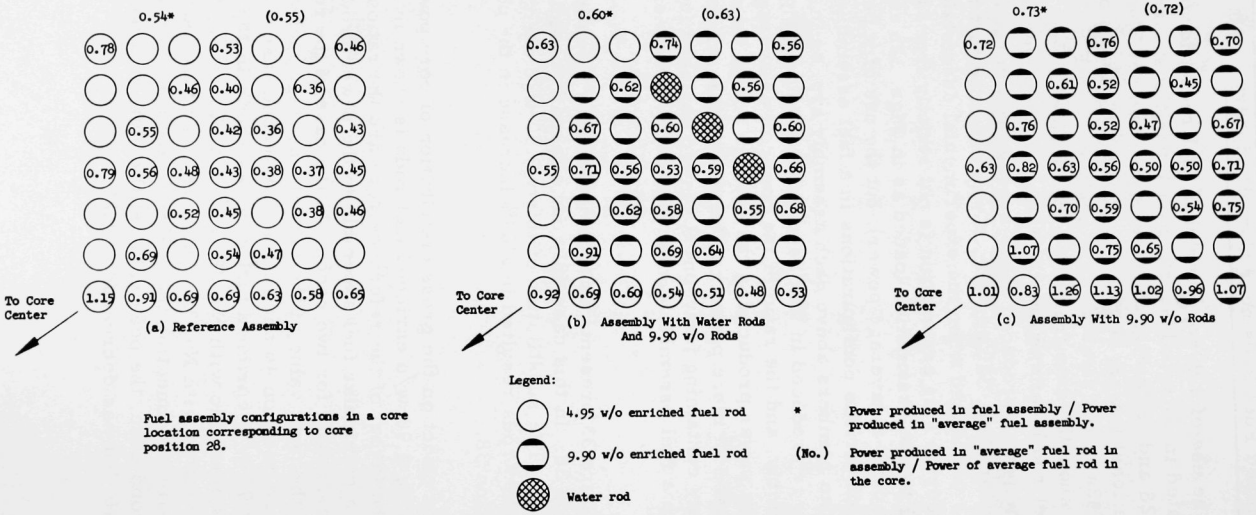

Fig. 32. Local-to-core-averaged Fuel Rod Power Distribution in Core B-1B

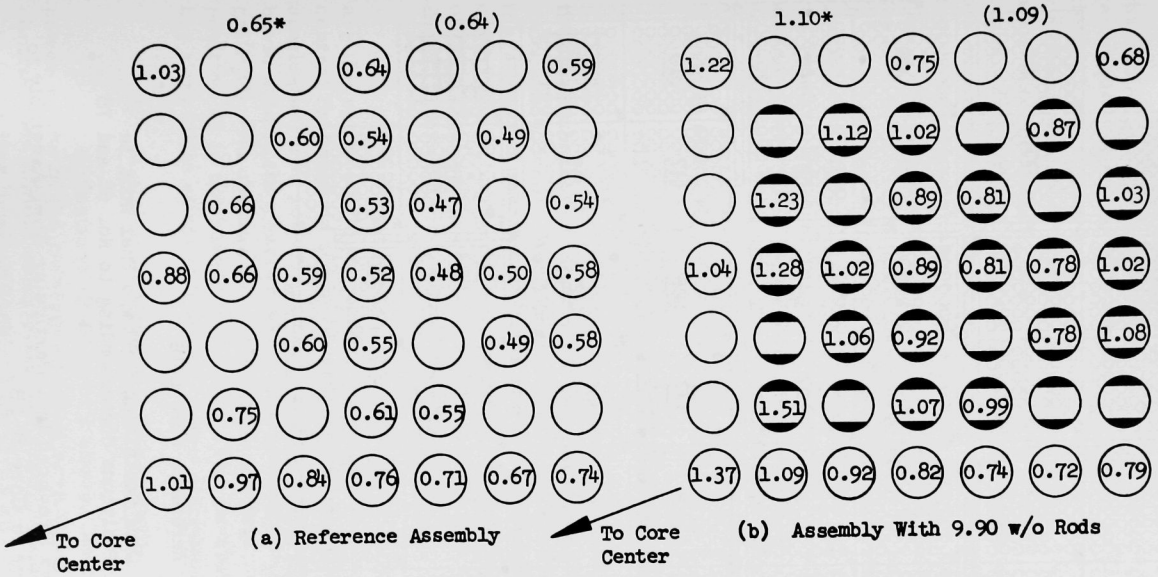

Fuel assembly configurations in a core location corresponding to core position 38.

Legend:

4.95 w/o enriched fuel rod

9.90 w/o enriched fuel rod

* Power produced in fuel assembly/Power produced in "average" fuel assembly.

(No.) Power produced in "average" fuel rod in assembly/Power of average fuel rod in the core.

Fig. 33. Local-to-core-averaged Fuel Rod Power Distribution in Core B-1A

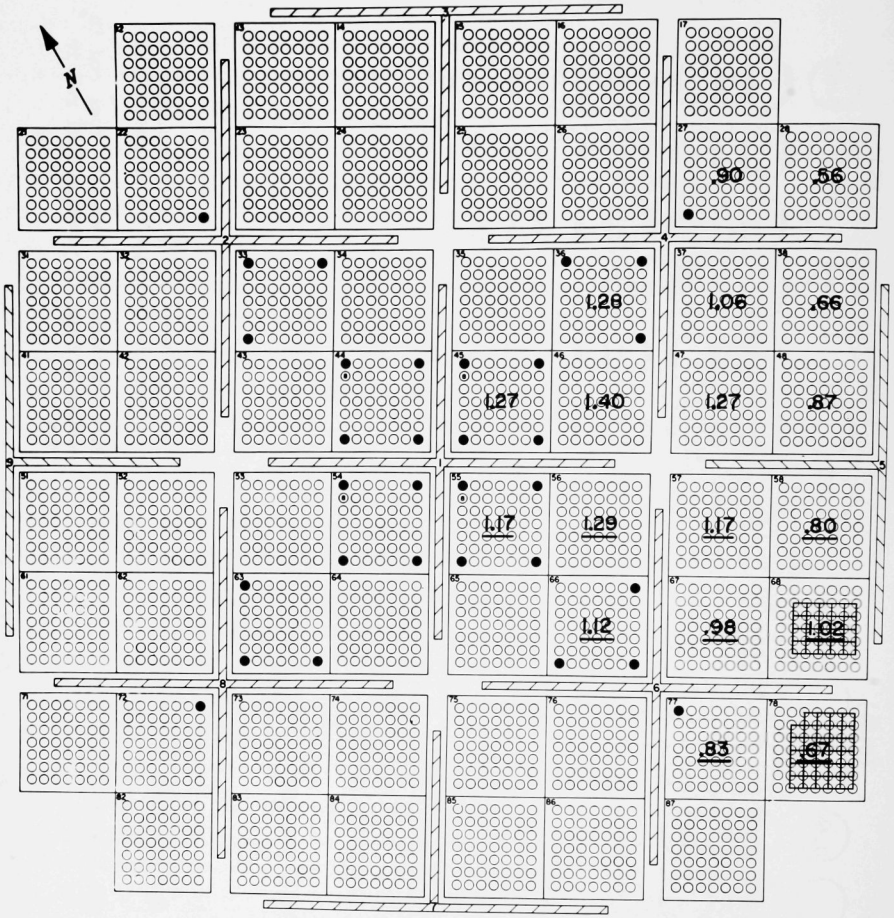

Plain Numbers: Reference Core B-1B

Underlined Numbers: Core Containing 9.90 w/o Fuel Rods in Positions Corresponding to No. 68 and 78

Fig. 34. Ratio of Power Produced in a Particular Fuel Assembly to Average Power in Core B-1B

d. Power Distribution Adjacent to a Control Rod

An investigation of the effect of a single control rod on the radial flux shape was made with core B-1A by the fine-flux-measuring technique. The flux-wire trays were placed in assemblies in core positions 45 and 46 at a height of 12 in. above the base of the fuel. Control rod No. 1 was inserted to 8 in. while all other control rods were banked at 18 in. The results, presented in Fig. 35, are in the form of ratios of the power produced in a fuel rod with the control rods positioned as stated above, to the power produced in the same fuel rod with all the control rods banked at about 22 in., which was the case when the data for Fig. 29 were obtained. The ratios are normalized to a value of 1.00 for the fuel rod farthest from the central control rod (fuel rod location No. 7 in core position 46), since the flux at this fuel rod is least affected by the control rod. It should be borne in mind that the numbers in Fig. 35 are not relative flux shapes in the two assemblies with the control rod inserted. The relative flux shape may be obtained by multiplying the numbers shown in Fig. 35 by the number for the corresponding fuel rod in Fig. 29. The symmetry in each side of the diagonal in core position 45 is good to about 4%.

e. Effect of Boric Acid Concentration on Power Distribution

The effect of boric acid on the fine-flux distribution within fuel assemblies near the core center was investigated. Measurements were made in core B-1B in core positions 45 and 46 with the flux-wire trays located near the vertical center of the unrodded core region in each case. The actual vertical location of the flux-wire trays differed because of the difference in height of the unrodded core region due to the greater insertion of control rods for the clean core.

The results are shown in Fig. 36. The numbers in Fig. 36 are the ratios of (1) the single-fuel-rod power/average power for the five central fuel rods in the particular assembly without boric acid to (2) the single-fuel-rod power/average power for the five central fuel rods with boric acid in the reactor water at a concentration of 18.52 $g(H_3BO_3)/gal(H_2O)$. No obvious pattern governs the data. The symmetry in core position 45 is not particularly good. The conclusion is that boric acid has very little effect on the fine-power distribution.

3. Maximum-to-average Power Ratio

In Sections III.D.1 and 2 above, the measured peak-to-average power ratios in the reference boiling core B-1B at room temperature, with control rods almost completely withdrawn, were 1.39 axially, and 1.99 radially (including local peaking). This gives an overall core maximum-to-average power ratio of 2.77. These measurements may be compared with estimated values[1] of 1.33 axially, 1.5 radially, and 1.3 for local peaking. The estimated overall maximum-to-average power ratio was 2.59.

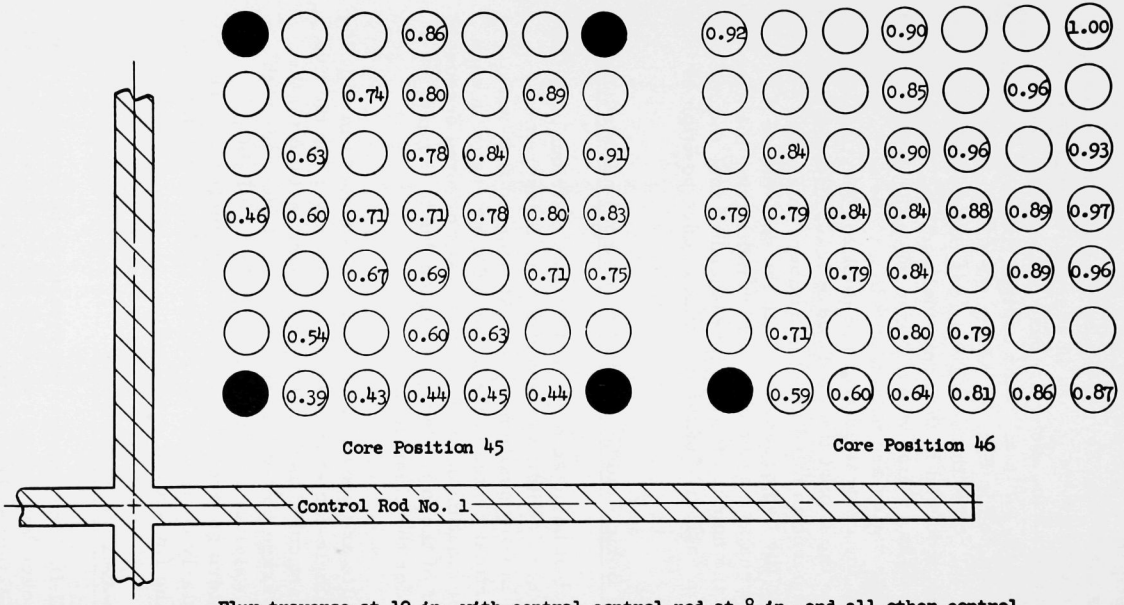

Flux traverse at 12 in. with central control rod at 8 in. and all other control rods banked at 18 in.

Legend:

(No.) **Power produced in fuel rod with central control rod inserted as indicated/ Power produced in fuel rod when all rods are banked about 10 in. above traverse plane. Normalized to fuel rod farthest from control rod. All fuel rods 4.95 w/o enriched.**

Boron-stainless steel rod

Fig. 35. Effect of Control Rod on Power Distribution in Adjacent Fuel Assemblies of Core B-1A

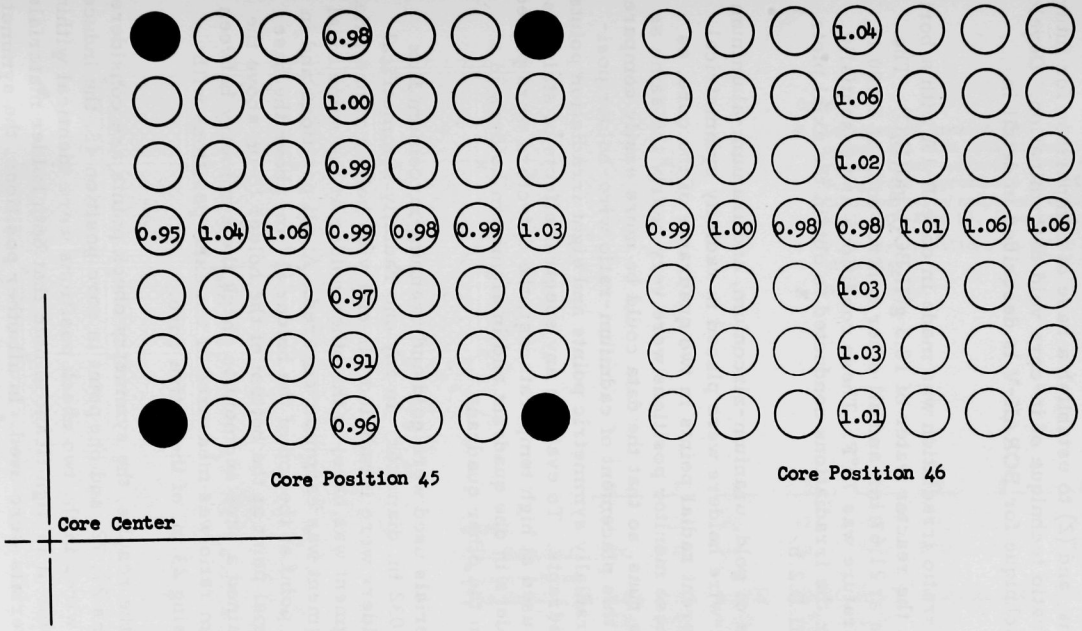

Fig. 36. Effect of Boric Acid on Fine-flux Distribution in Core B-1B

E. Cadmium-ratio Measurements

Cadmium-ratio measurements were made at zero power with the boiling core for two reasons: (1) to measure neutron-flux spectrum in various core locations, and (2) to establish a base of comparison for future use of the cadmium-ratio technique of in-core void determination. Development of this latter technique for BORAX-V is described in detail in ANL-6620.[5]

The cadmium-ratio irradiation was made in core B-1A with a boric acid concentration in the reactor water of 18.3 $g(H_3BO_3)/gal(H_2O)$. The No. 1 control rod was at 21.67 in., and all other control rods at 21.00 in. Reactor water temperature was 70°F. These conditions are essentially the same as those for the irradiations conducted to obtain the axial plots reported in Section III.D.2.b.

Monitor wires of gold, uranium-zirconium, and uranium-aluminum were used. Two flux-wire holders were placed in radially symmetrical positions at four different radial points in two quadrants of the core, as shown in Fig. 37. These monitor positions were very nearly the same as those for all previous runs, so that the data could be more easily compared. As shown in Fig. 37, this placement of cadmium-ratio wire-holder positions results in four radially symmetric points and eight irradiation points in each of the two quadrants. To evaluate any spectral effects of stainless steel thimbles (to be used at high temperatures), the detectors were placed in stainless steel holders in one quadrant and in aluminum holders in a symmetric position in the other quadrant.

Detector materials used were gold and uranium-zirconium flux wires, $\frac{3}{8}$ in. long x 0.032 in. diameter. In any one radially symmetrical position, two wire holders were irradiated. In one wire holder at one axial location, the wire segment was bare; in the other holder at the same axial location, the wire segment was cadmium-covered. At all positions and in all holders, one axial point at the top of the holder (17 in. above the base of the fuel) and one axial point at the bottom of the holder (5 in. above the base of the fuel) contained a bare segment to check the symmetry between holders. The cadmium ratio was measured at ten axial positions with 2-in. spacing, traversing 23 in. of the active core.

In discussing the results, the symmetry check points are considered first. In core positions 27, 72, and one point in core position 45, the induced activities of the bare wires in the two check positions were identical within 1%, both top and bottom. It is significant to note that both holder materials and both detector materials were used. In all other positions, the symmetry check points did not compare so well, and the deviations varied from 3 to 11%. In all but two cases, one in core position 36 and one in core position 54,

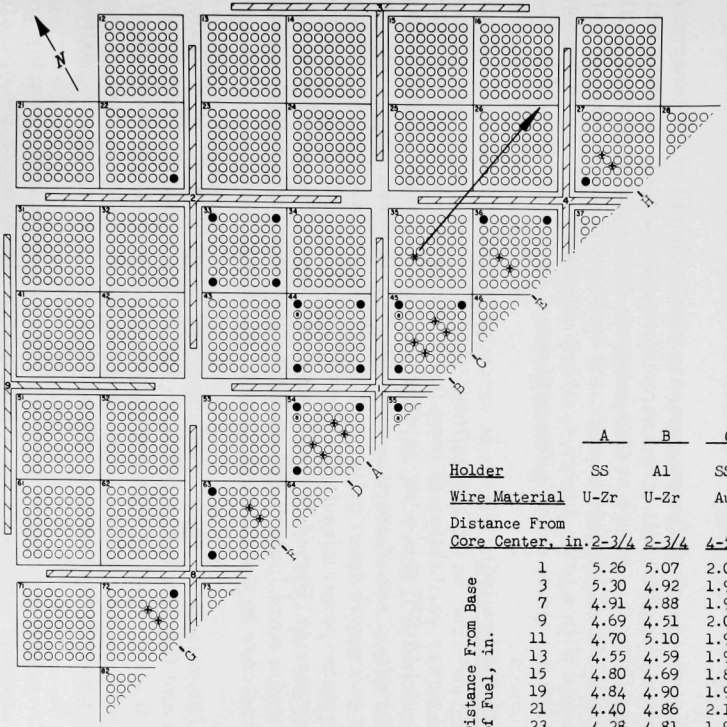

Code:

- * Location of uranium foil for comparison with foil at reactor vessel inner surface. Arrow designates approximate direction of comparative sample at vessel wall (70° E of N). (See text.)
- \+ Flux wire positions in water channels.
- ● Poison rods.

		A	B	C	D	E	F	G	H
Holder		SS	Al	SS	Al	SS	Al	SS	Al
Wire Material		U-Zr	U-Zr	Au	Au	U-Zr	U-Zr	Au	Au
Distance From Core Center, in.		2-3/4	2-3/4	4-5/32	4-5/32	8-3/8	8-3/8	15-5/32	15-5/32
Distance From Base of Fuel, in.	1	5.26	5.07	2.03	2.27	4.20	5.15	1.81	2.34
	3	5.30	4.92	1.97	2.06	4.15	4.72	2.31	2.05
	7	4.91	4.88	1.90	2.17	4.63	4.73	1.98	2.04
	9	4.69	4.51	2.01	2.04	4.33	4.46	2.09	2.03
	11	4.70	5.10	1.93	2.33	4.41	4.61	2.17	2.08
	13	4.55	4.59	1.99	2.04	4.67	4.49	1.28	2.04
	15	4.80	4.69	1.89	2.12	4.42	4.30	2.06	2.03
	19	4.84	4.90	1.91	2.12	4.39	4.66	2.12	1.93
	21	4.40	4.86	2.10	2.06	4.30	4.93	1.89	1.95
	23	4.28	4.81	1.90	2.29	4.38	5.09	2.06	1.92

Fig. 37. Cadmium-ratio Survey of Core B-1C

the deviation was the same top and bottom, 5% or less. Consideration of the uncertainties of lateral positioning in the severe flux gradient of the water channels leads to the conclusion that a deviation of 5% is reasonable. The two cases for which the deviation was greater than 5% and not consistent top to bottom, are difficult to explain except as poor data. In both of these cases, the detector material was uranium-zirconium alloy and the results are not reported.

The cadmium ratios presented in Fig. 37 were computed by a normalization procedure involving two holders at one radial point. The activities of the bare segments of one holder were normalized to the peak value for the axial traverse, and then the activities of the bare segments of the other holder were normalized to this curve at one of the symmetry check points. The activity of a bare segment as read from the curve was then applied, and the activity of a cadmium-covered segment measured at the same point was used to compute the ratio. This normalization procedure was also applied to the observed count for the cadmium-covered segment.

A cadmium-ratio measurement was also made at the inner surface of the reactor vessel shell in the same aluminum capsule with the foils used to measure flux levels at that point, as discussed in Section III.D.1.c. The location of this capsule is indicated on Fig. 37. The cadmium ratio, as measured with a bare, highly enriched uranium foil and a foil covered with a 0.020-in. thickness of cadmium, was 2.72.

F. Power Calibration

A power calibration of core B-1A was performed, by irradiating a highly enriched U^{235} flux wire, to determine the absolute number of fissions. To obtain satisfactory count rates on flux wires, the reactor was operated at a power level calibrated at 300 w. At this power level, the linear neutron-power circuit, Channel III, read 0.5×10^{-5} amp, and the log power circuit, Period I, read 0.48×10^{-5} amp. The chambers for these circuits were located in 5-in.-diameter aluminum thimbles just outside the core in the reflector, as shown in Fig. 9.

The calculated relationship between the total number of fissions in the core and fissions in the U^{235} wire included a correction factor for neutron-flux level at the wire compared with the average radial flux level in the core based on other flux-wire irradiations. The correction factor for axial flux distribution was estimated, based on control rod position.

Irradiations made with boric acid in solution in the reactor coolant were performed at the same apparent neutron-flux level on the operating instruments. The actual power level with boric acid, due to the change in ratio of the flux at the instruments to the flux in the core because of boric acid, was estimated to be about 900 w.

G. Oscillator-rod Experiments

Following the flux measurements, experiments were carried out with core B-1C to determine the optimum location in the reactor vessel of the oscillator-rod assembly which had been designed and built for use in transfer function experiments during operation of BORAX-V. The oscillator rod is shown disassembled in Fig. 38. The photograph of the oscillator is disjointed in that the two portions on the left are extensions of the two portions on the right and are actually joined to them. The rotor and drive shaft are inserted into the stator and shaft housing, and held in position by the two bearings at the top and bottom of the stator. A shaft from the drive motor is connected above the seal. During operation, the speed of the rotating oscillator can be varied from about 0.4 to 1100 rpm. During power operation of the reactor, the seal housing can be connected to any one of the three oscillator nozzles in the head of the reactor vessel, with the stator located in thimble C outside the core or in core position 85 or 75, depending on which nozzle is used (see Fig. 10 for locations).

The rotor of the oscillator is an annular tube which contains a 165° arc of Boral (inside radius of 1.112 in.; 0.047 in. thick) clad with Zircaloy-2. The length of the poison section is 28 in., and it is possible to raise the oscillator so that only a portion of the poison length is inserted into the core. During operation, the poison section rotates through the flux gradient and produces a periodic reactivity change.

The differential reactivity worth of the oscillator was not known at the start of the experiments, but the oscillator rod had been designed to have as large an effect as possible for the maximum size of rotor that would fit into a fuel-assembly position. The differential effect was known to be a function of position in the vessel, and it was desirable to place the oscillator rod outside the core, in thimble C. This location was tried first; the total effect of the oscillator was found to be -0.131% $\Delta k/k$, and the differential effect was found to be 0.012% $\Delta k/k$, peak-to-peak. The oscillator-rod assembly was next placed in core position 85, with a resulting total effect of -0.404% $\Delta k/k$ and a differential effect of 0.035% $\Delta k/k$. The oscillator-rod assembly was next placed in core position 75. In order to minimize flux peaking in fuel assemblies adjacent to the dummy fuel assembly which held the stator, the corners of the dummy fuel assembly were filled in with aluminum. The differential reactivity effect in this position was insufficient, and attempts were made to increase the differential worth through various means. The results of the investigation in core position 75 are shown in Table I. Figure 39 is a cross section of the final configuration, which included three fuel rods in each corner of the modified fuel assembly box which locates the stator and a 165° arc of 2 w/o natural boron-stainless steel located away from the core center. Figure 40 is a photograph of this assembly. As indicated in Table I, the final configuration in core B-1B' resulted in a total reactivity effect of -0.75% and a differential effect of 0.12%.

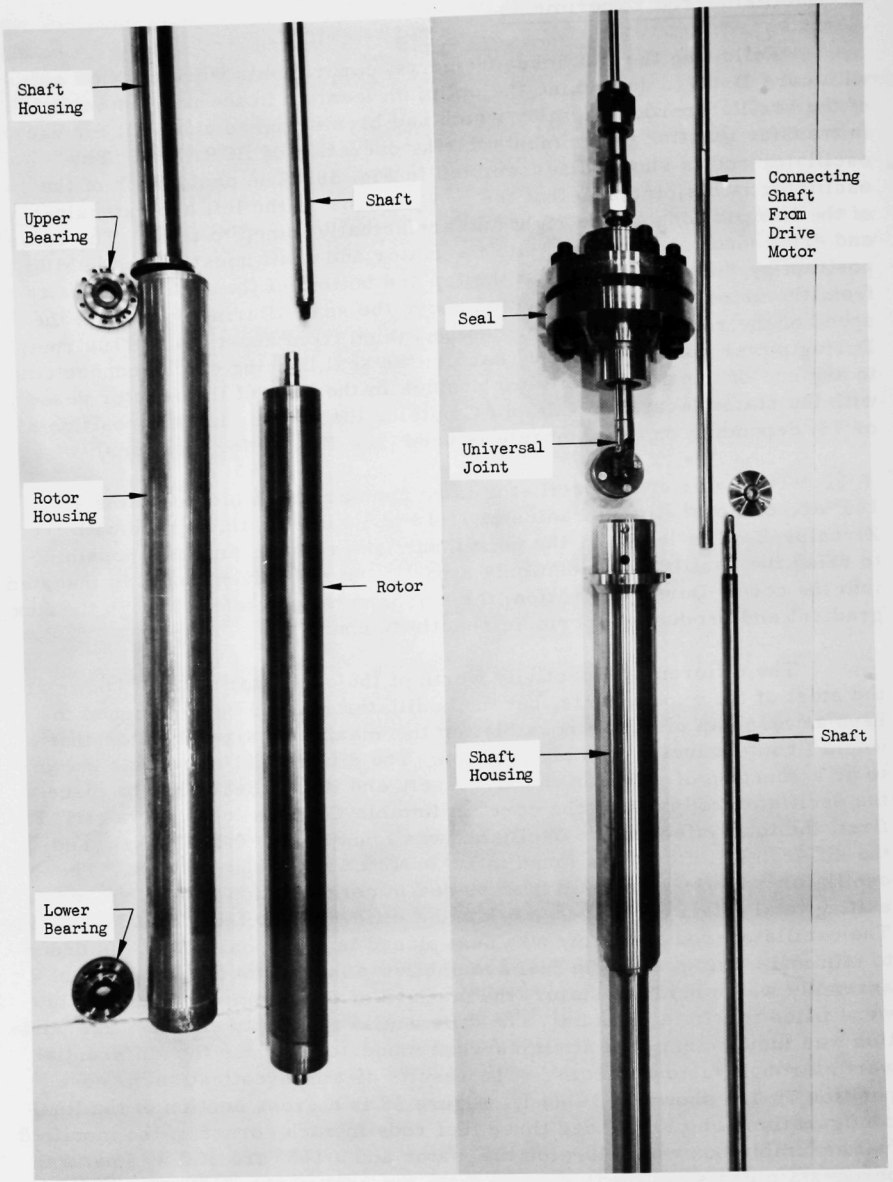

Fig. 38. Disassembled Oscillator Rod

Table I

REACTIVITY EFFECTS OF VARIOUS ROTATING OSCILLATOR-ROD CONFIGURATIONS FOR CORE POSITION NO. 75

Poison Arc (degrees)	Poison Thickness and Material		Peak-to-peak Reactivity Differential Effect (%)	Total Reactivity Effect* (%)	Remarks
	Rotor	Stator			
165	0.147-in. 50 w/o B_4C Boral, clad with 1/16-in. Zircaloy-2	None	0.055	-1.3	Aluminum filler pieces in all four corners of oscillator assembly
165	"	None	0.047	-1.3	Water in two corners of oscillator assembly toward core center
165	"	None	0.074	-1.3	Water in two corners of oscillator assembly away from core center
165	"	0.020-in. cadmium	0.10	-1.3	Aluminum filler pieces in all four corners of oscillator assembly
165	"	"	0.10	-1.3	Water in two corners of oscillator assembly away from center
60	0.040-in. cadmium	0.040-in. cadmium	0.05	-0.8	Aluminum filler pieces in all four corners of oscillator assembly
90	"	"	0.07	-0.8	Aluminum filler pieces in all four corners of oscillator assembly
165**	0.147-in. 50 w/o B_4C Boral, clad with 1/16-in. Zircaloy-2	0.020-in. cadmium	0.12	-0.75	Three 5% fuel rods in each corner of oscillator assembly

*This is the total reactivity effect due to replacing the boiling fuel assembly with the oscillator assembly. Rotor and stator poisons adjacent to one another, pointing away from core center.

**This is the final configuration adopted for use, except that the cadmium was replaced with 0.125-in.-thick, 2-w/o natural boron-stainless steel.

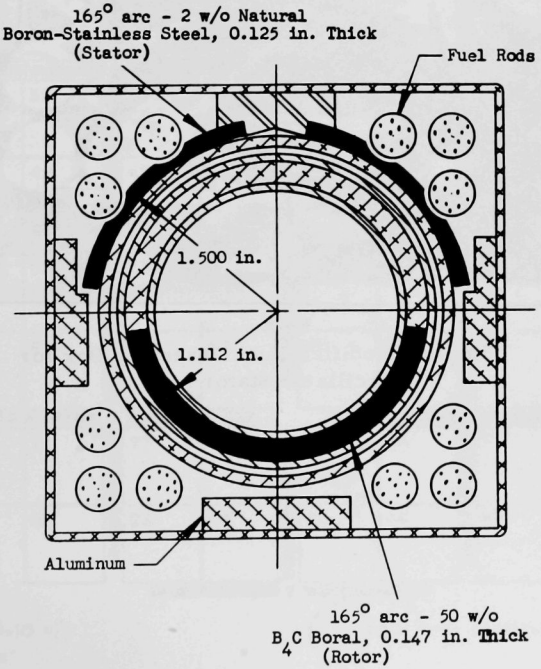

Fig. 39. Section through Oscillator Rod

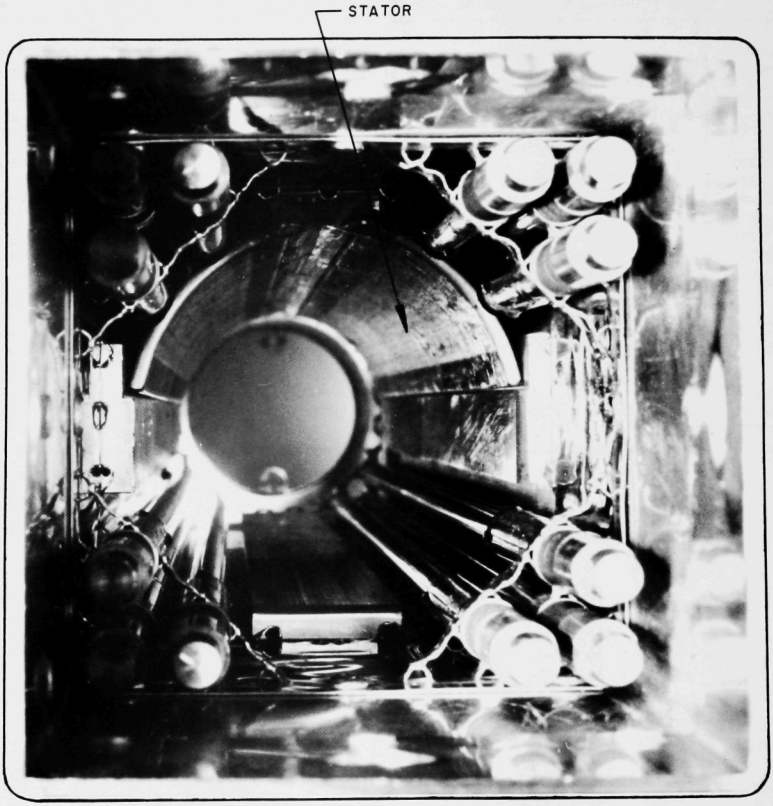

Fig. 40. Modified Fuel Assembly Box for Oscillator Stator

IV. ROOM-TEMPERATURE AND HIGH-TEMPERATURE EXPERIMENTS WITH CORE B-1D

The B-1B core configuration was modified to core B-1D, as shown in Fig. 41, as follows: (a) a standard fuel assembly was removed and the oscillator assembly inserted; (b) six $\frac{1}{8}$-in.-diameter stainless steel flux-wire thimbles were inserted; (c) four fuel rods were removed and four stainless steel, $\frac{3}{8}$-in.-diameter miniature ion-chamber thimbles inserted; and (d) one fuel rod was removed and one special, fixed, miniature ion chamber in a special, short, $\frac{3}{8}$-in.-diameter stainless steel holder inserted. The results of Section III.C.5 imply that the reactivity effect of (b), (c), and (d) was about -0.1%.

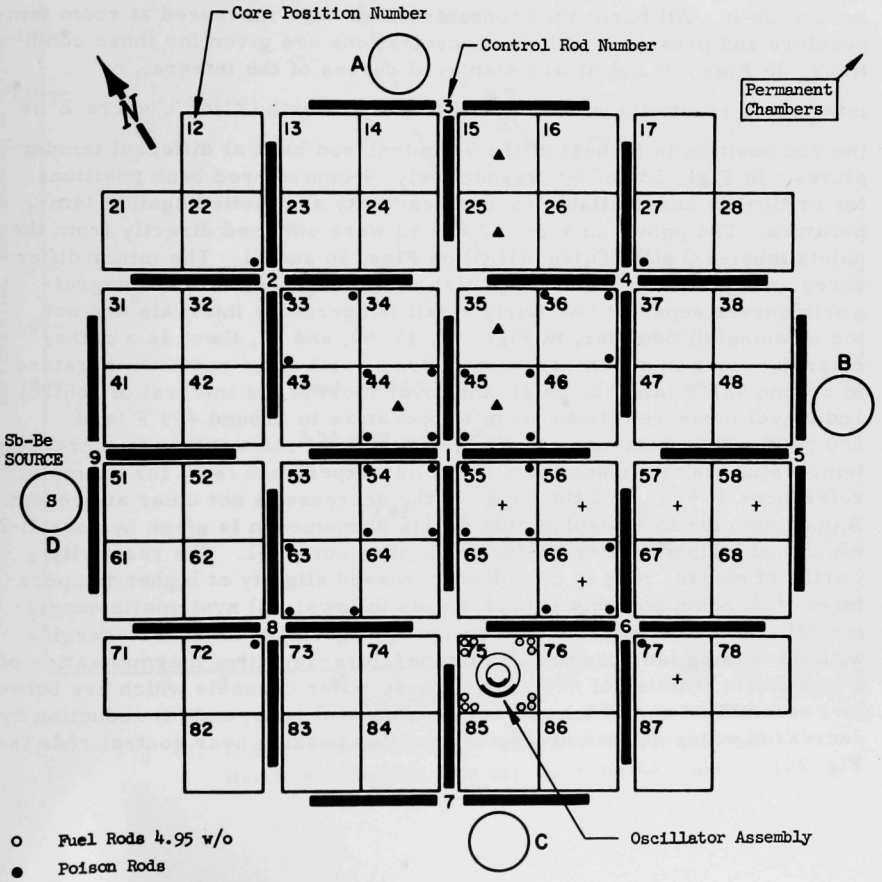

Fig. 41. Boiling Core B-1D

At temperatures above ~150°F, control rod drive and pump seal water flows into the reactor vessel, and leak-off water may be returned to the feedwater tank. In order to maintain a fairly constant boric acid concentration in the reactor vessel, the boric acid concentration in the feedwater tank was made nearly equal to the concentration in the reactor vessel.

A. Control Rod Worths

In Figs. 42-49 are displayed differential reactivity worth curves for various control rods and combinations of control rods at different temperatures. Several of the curves have been extended arbitrarily to zero at 26 in. All boric acid concentrations were measured at room temperature and pressure, and all concentrations are given for these conditions. In Figs. 50 and 51 are displayed curves of the integral, or integrated, reactivity worth ($\int_Z^{26}$ differential worth $(Z')dZ'$, where Z' is the rod position in inches) of the 9-control-rod bank at different temperatures. In Figs. 52 and 53, respectively, 9-control-rod bank positions for criticality and available excess reactivity are plotted against temperature. The points on Figs. 52 and 53 were obtained directly from the points labeled O $g(H_3BO_3)/gal(H_2O)$ on Figs. 50 and 51. The minor differences among some of the differential and among some of the integral-worth curves separated by fairly small temperature intervals are not too meaningful; however, in Figs. 42, 43, 50, and 51, there is a rather clear decrease in differential control rod worth from room temperature to around 421°F (and 300 psig) and, over most of the interval of control rod travel measured, from room temperature to around 489°F (and 600 psig). This decrease of differential control rod worth with increasing temperature is not in accord with earlier experience (see, for example, references 3, 6, 7), and the cause of the decrease is not clear at present. A possible clue to an explanation of this phenomenon is given by core B-2, which had a higher water-to-fuel ratio than core B-1. The reactivity worths of control rods in core B-2 increased slightly at higher temperatures.[10] Some possible causes are as follows: (a) systematic experimental errors, (b) shift of neutron-energy spectrum to higher energies with increasing temperature, (c) temperature-sensitive thermalization of a significant fraction of neutrons in those water channels which are between fuel assemblies and which are not near control rods, and (d) reduction by decreased water density of the thermal flux peaking near control rods (see Fig. 26).

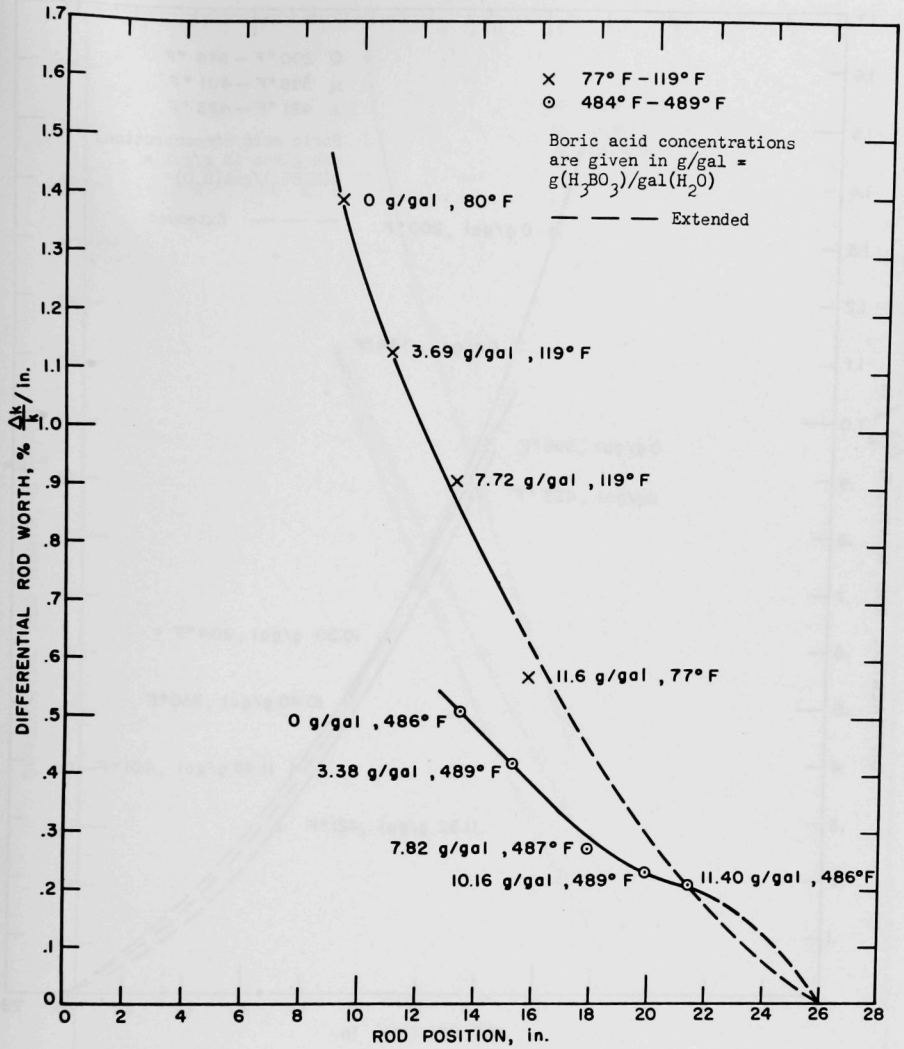

Fig. 42. Differential Reactivity Worth of 9-control-rod Bank vs. Rod Position for Core B-1D, Part I

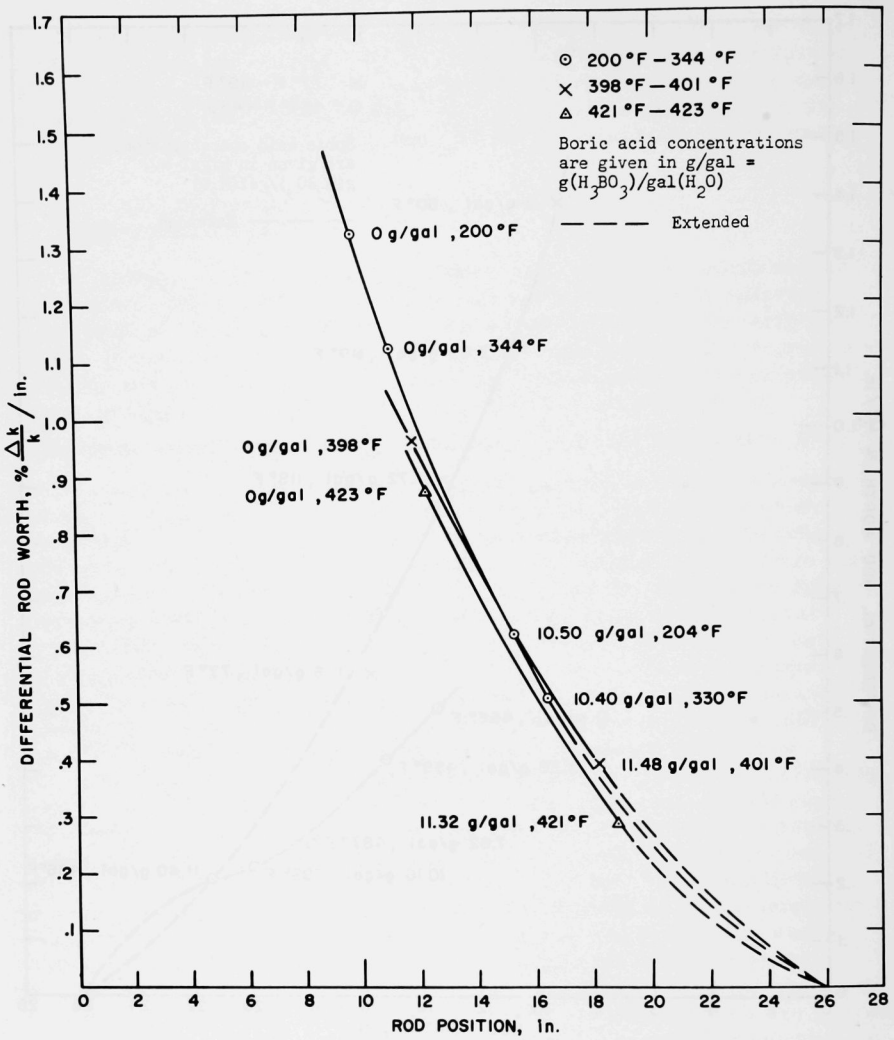

Fig. 43. Differential Reactivity Worth of 9-control-rod Bank vs. Rod Position for Core B-1D, Part II

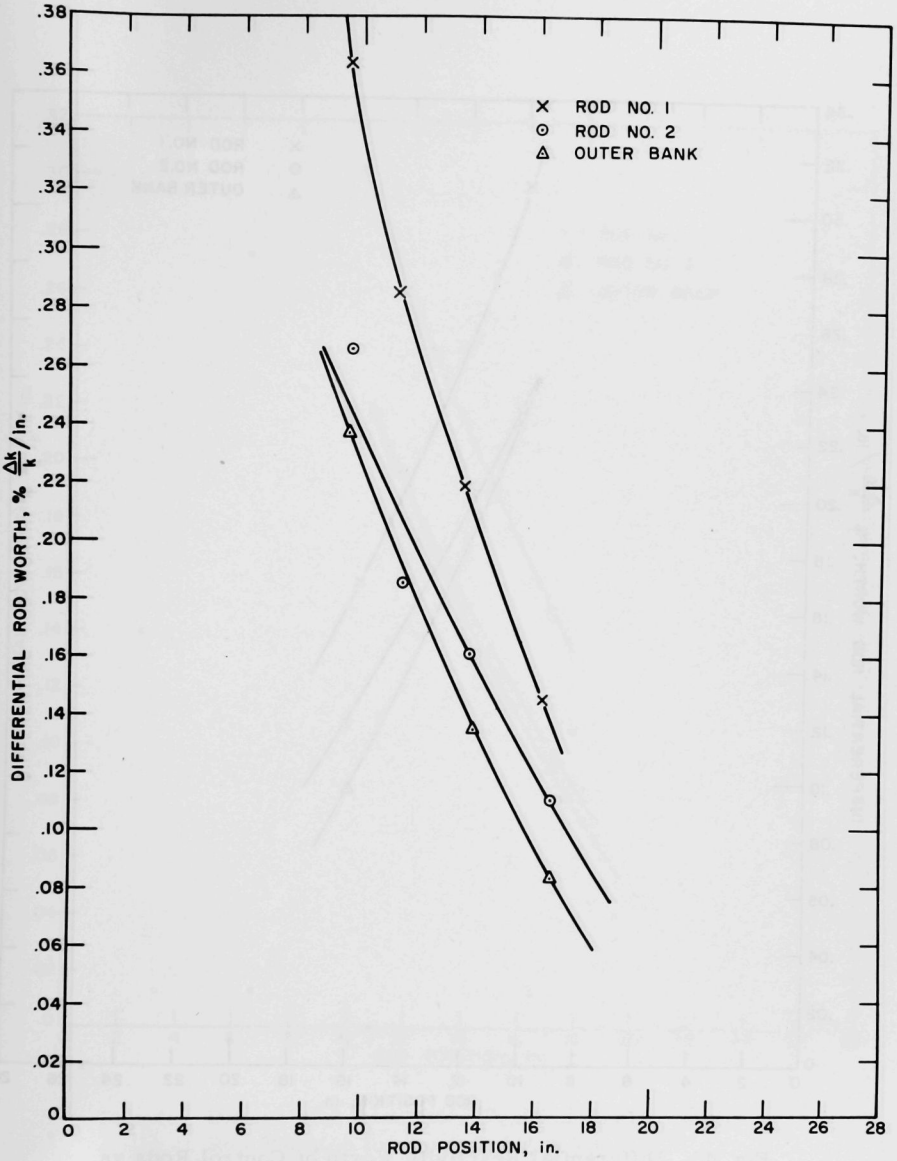

Fig. 44. Differential Reactivity Worth of Control Rods vs. Rod Position for Core B-1D at 77-119°F

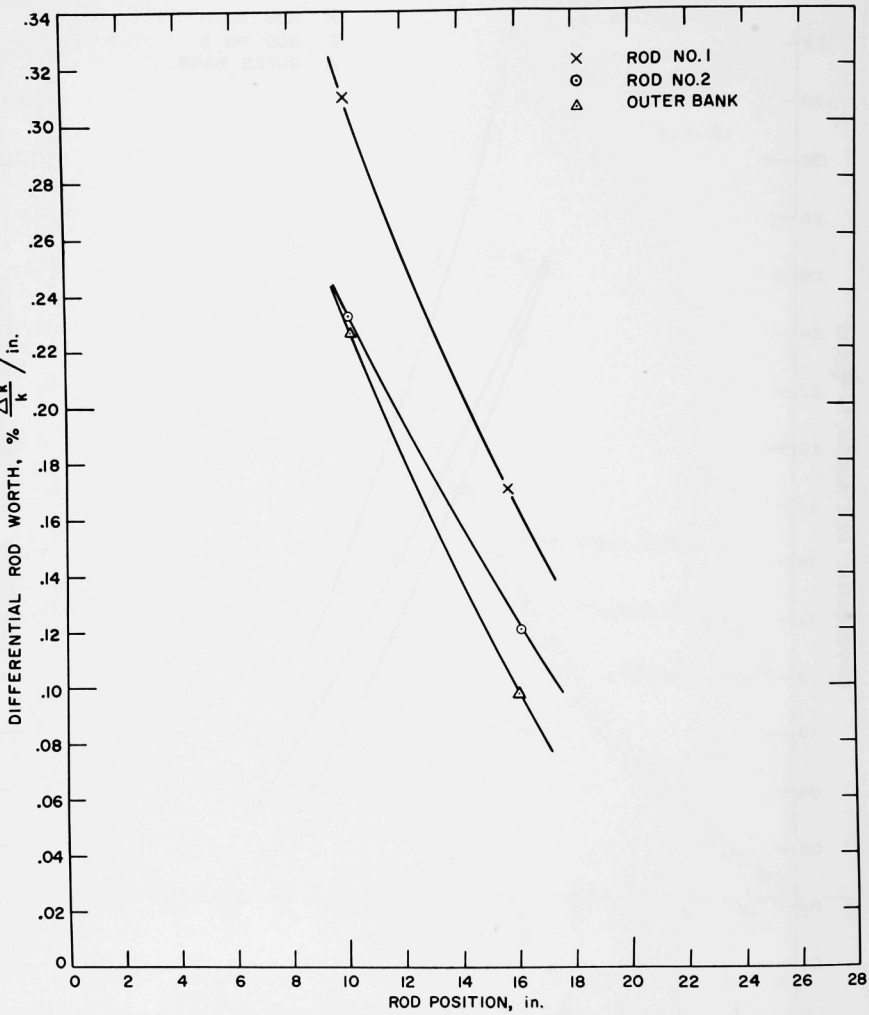

Fig. 45. Differential Reactivity Worth of Control Rods vs. Rod Position for Core B-1D at 200-208°F

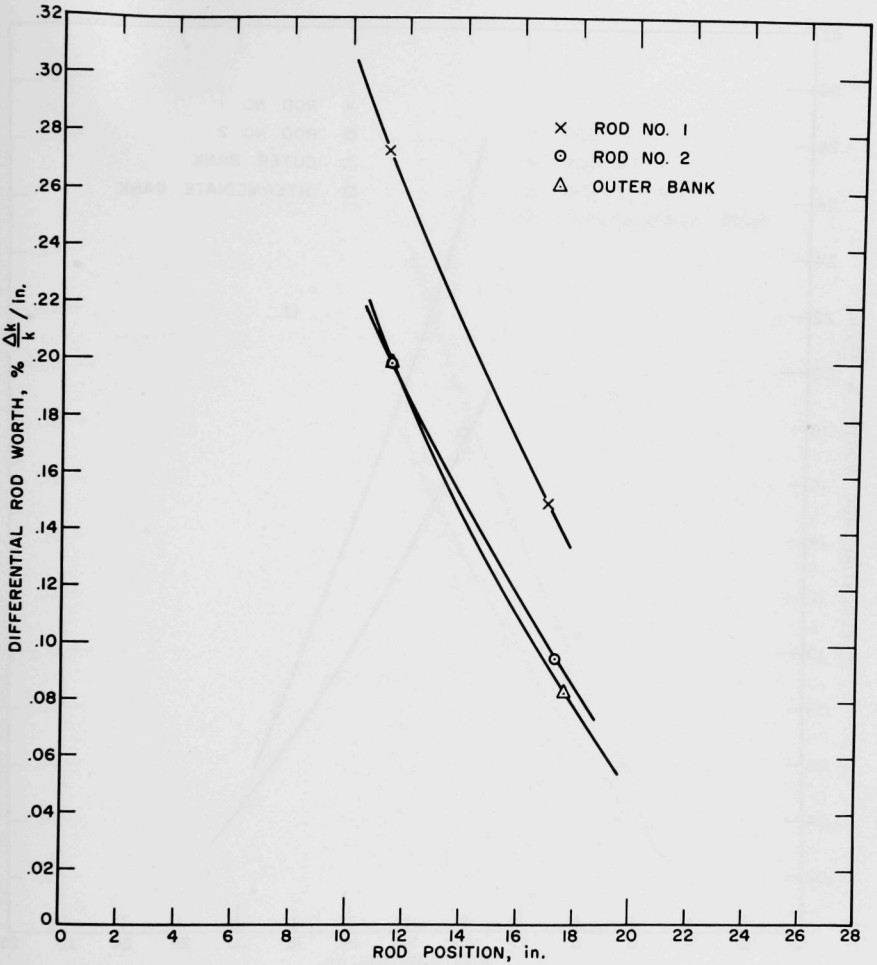

Fig. 46. Differential Reactivity Worth of Control Rods vs. Rod Position for Core B-1D at 330-344°F

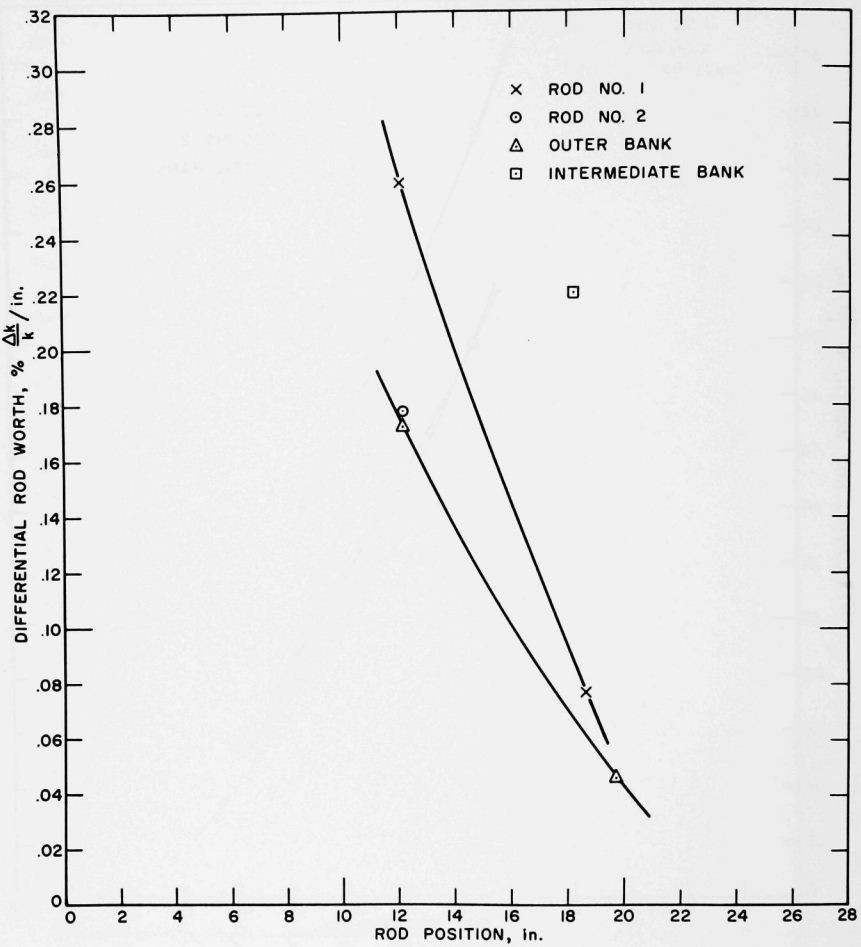

Fig. 47. Differential Reactivity Worth of Control Rods vs. Rod Position for Core B-1D at 396-401°F

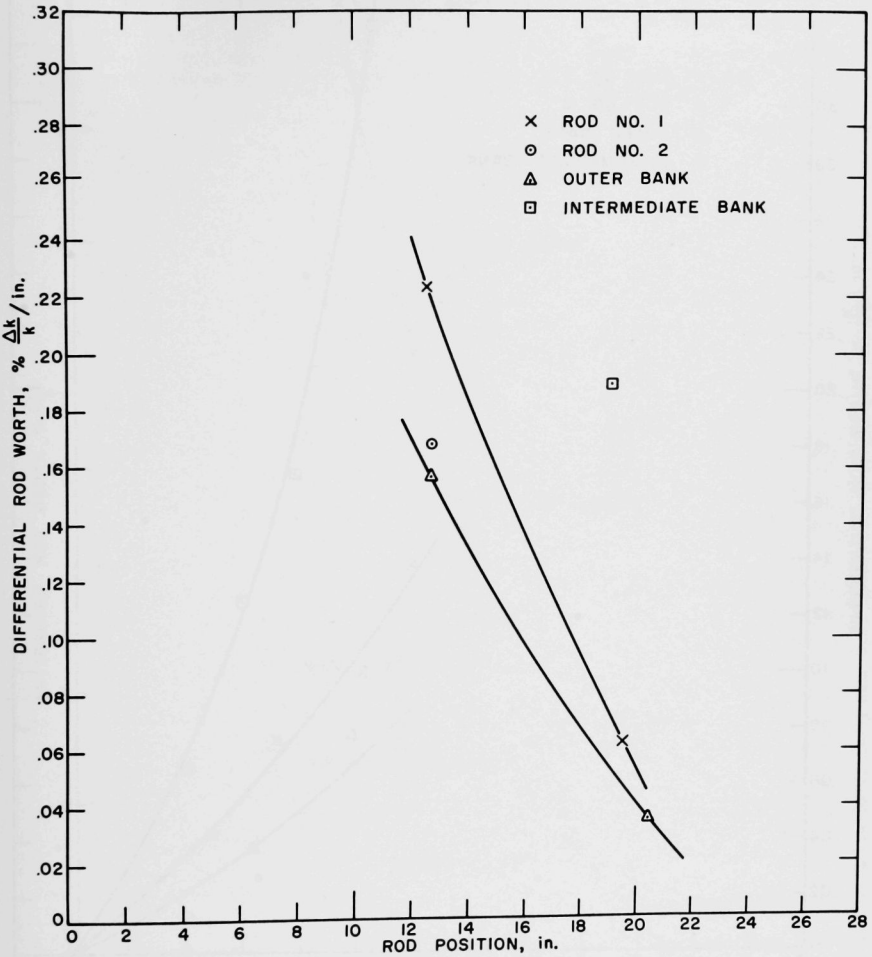

Fig. 48. Differential Reactivity Worth of Control Rods vs. Rod Position for Core B-1D at 421-425°F

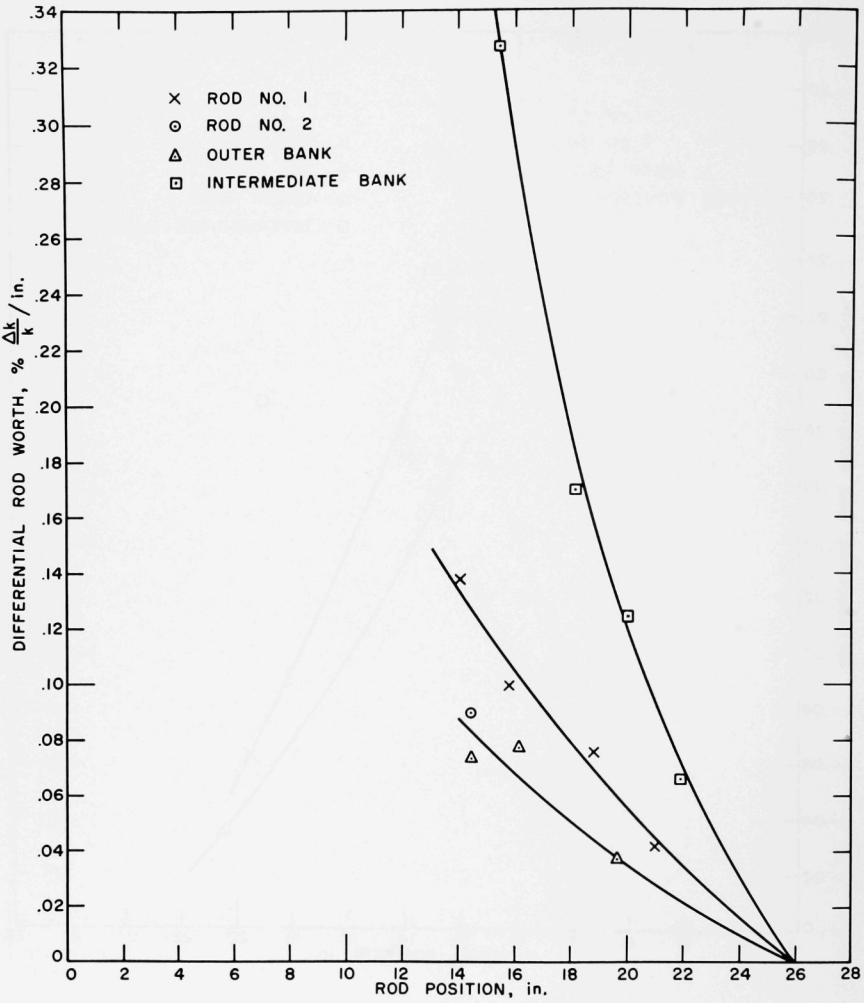

Fig. 49. Differential Reactivity Worth of Control Rods vs. Rod Position for Core B-1D at 483-490°F

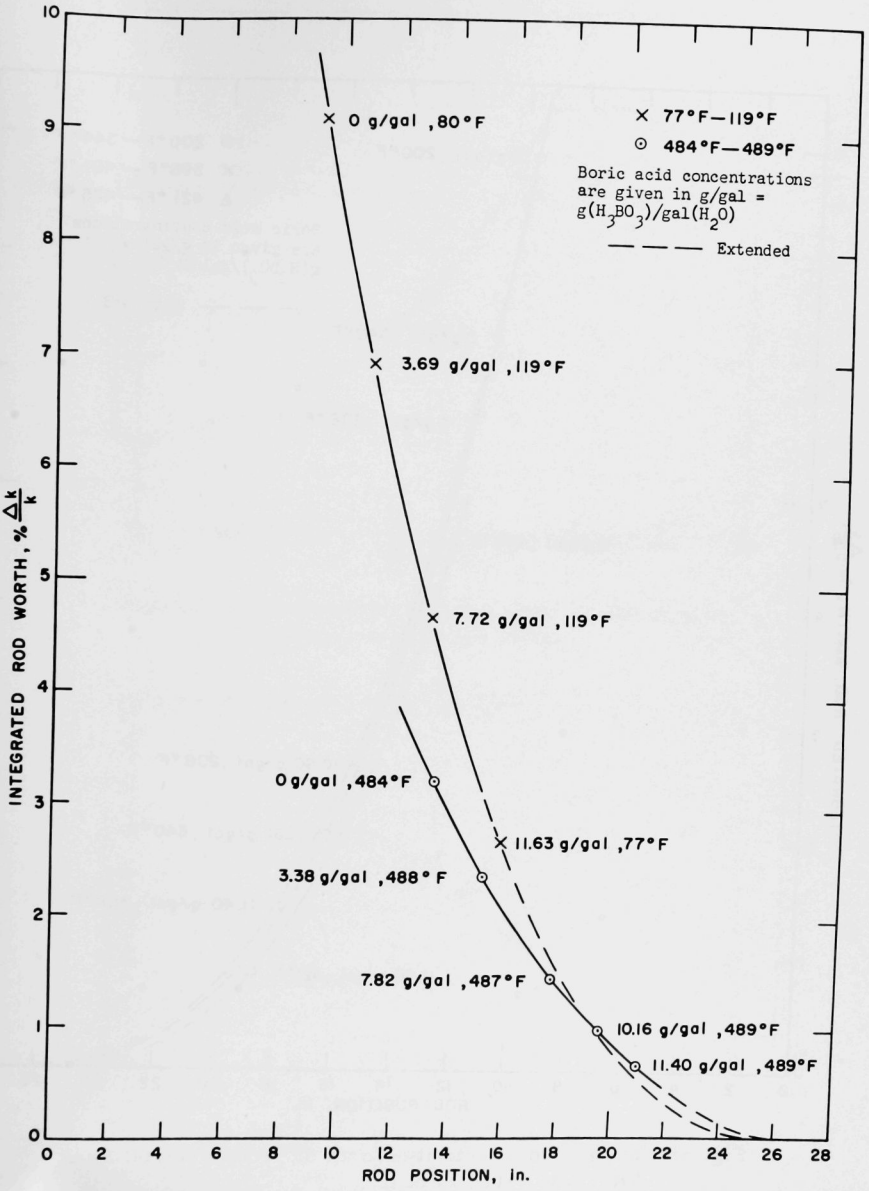

Fig. 50. Integrated Reactivity Worth of 9-control-rod Bank for Core B-1D, Part I

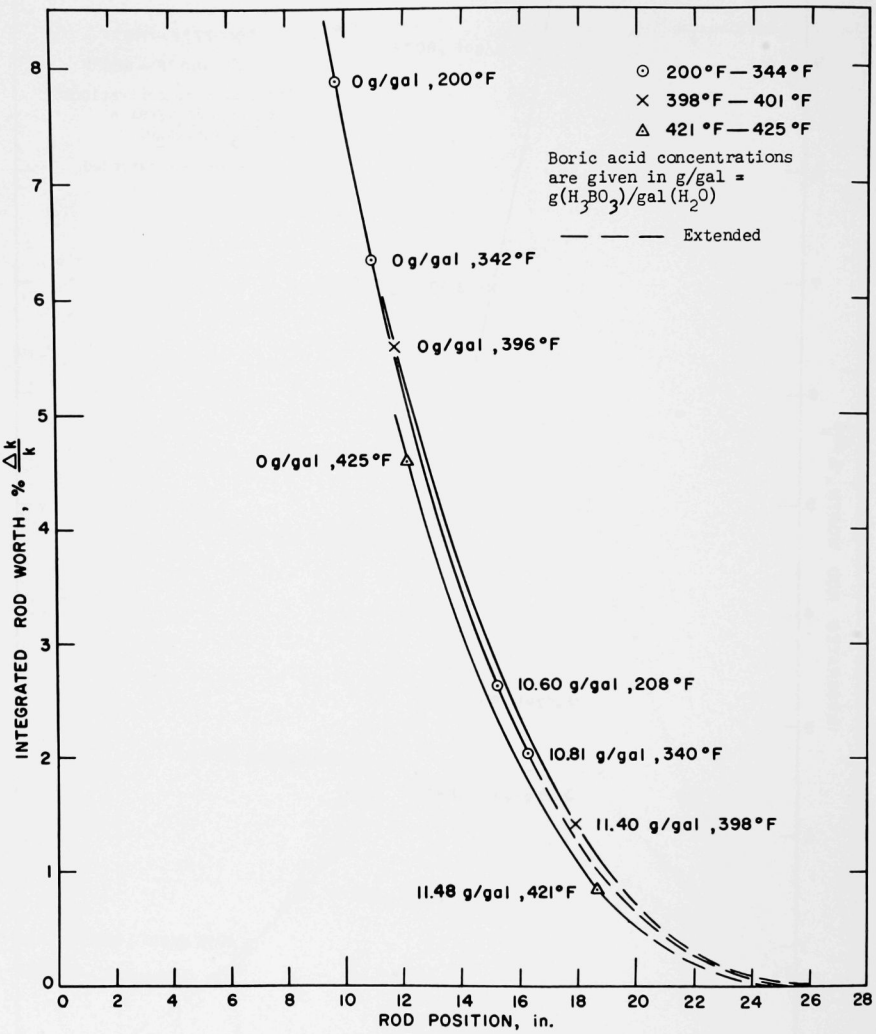

Fig. 51. Integrated Reactivity Worth of 9-control-rod Bank for Core B-1D, Part II

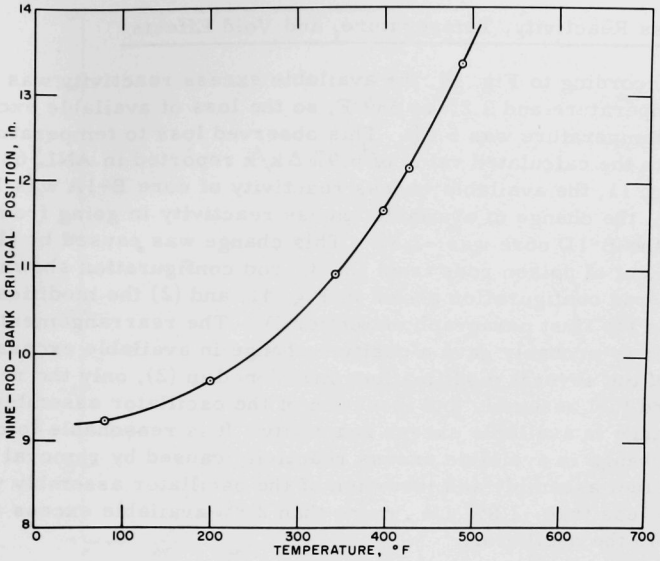

Fig. 52. Nine-control-rod Bank Critical Position vs. Temperature for Core B-1D

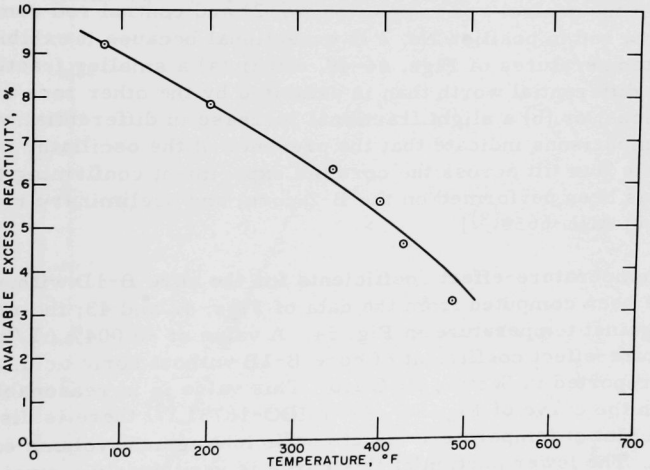

Fig. 53. Available Excess Reactivity vs. Temperature for Core B-1D

B. Excess Reactivity, Temperature, and Void Effects

According to Fig. 50, the available excess reactivity was 9.1% at room temperature and 3.2% at 489°F, so the loss of available excess reactivity to temperature was 5.9%. This observed loss to temperature compares with the calculated value of 6.9% $\Delta k/k$ reported in ANL-6302.(1) From Fig. 11, the available excess reactivity of core B-1A was 11.9%; therefore, the change of available excess reactivity in going from the core B-1A to the B-1D core was -2.8%. This change was caused by (1) the rearrangement of poison rods from the 36-rod configuration shown in Fig. 9 to the 32-rod configuration shown in Fig. 41, and (2) the modifications described in the first paragraph of Section IV. The rearrangement referred to in (1) very probably gave a positive change in available excess reactivity. Of the several modifications mentioned in (2), only the removal of a standard fuel assembly and insertion of the oscillator assembly caused much change in available excess reactivity. It is reasonable to conclude that the change in available excess reactivity caused by removal of a standard fuel assembly and insertion of the oscillator assembly was algebraically less than -2.8%, i.e., more than 2.8% available excess reactivity was lost to the oscillator.

Another effect attributable to the oscillator is revealed by numerical comparisons of results in Figs. 12 and 13 with results in Figs. 42-49. The modifications of core B-1D and new control rods have caused a decrease in differential reactivity worth, relative to core B-1A, of control rods (other than the control rod in position No. 2) and control rod combinations. The control rod in position No. 2 is exceptional because it exhibits, in the range of temperatures of Figs. 44-49, either (a) a smaller fractional decrease in differential worth than is exhibited by the other rods and rod combinations, or (b) a slight fractional increase in differential worth. These comparisons indicate that the presence of the oscillator caused an appreciable flux tilt across the core [an experiment confirming this conclusion has been performed on the B-2 core, and preliminary results are reported in ANL-6658(8)].

Temperature-effect coefficients for the core B-1D without boric acid have been computed from the data of Figs. 42 and 43; the results are plotted against temperature in Fig. 54. A value of -0.004% $\Delta k/k/°F$ for the temperature-effect coefficient of core B-1B without boric acid, at about 80°F, is reported in Section III.C.1.b. This value is in reasonable agreement with the curve of Fig. 54. As in IDO-16751,(9) there is displayed in Fig. 55 a plot of temperature effect coefficient against volume expansivity of water. The lower portion of this curve is very nearly a straight line with slope -0.22% $\Delta k/k$ per % void. This value is considerably smaller in magnitude than the -0.36% $\Delta k/k$ per % void reported in Section III.C.3.a. Some possible causes, other than experimental error, for the difference

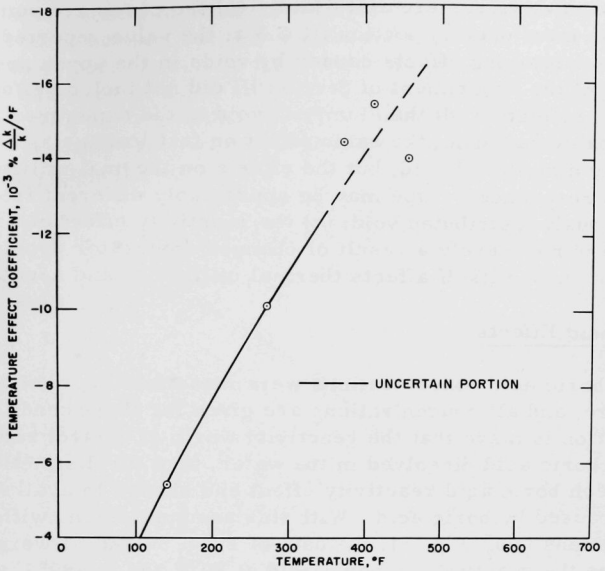

Fig. 54. Temperature-effect Coefficient of Reactivity vs. Temperature for Core B-1D

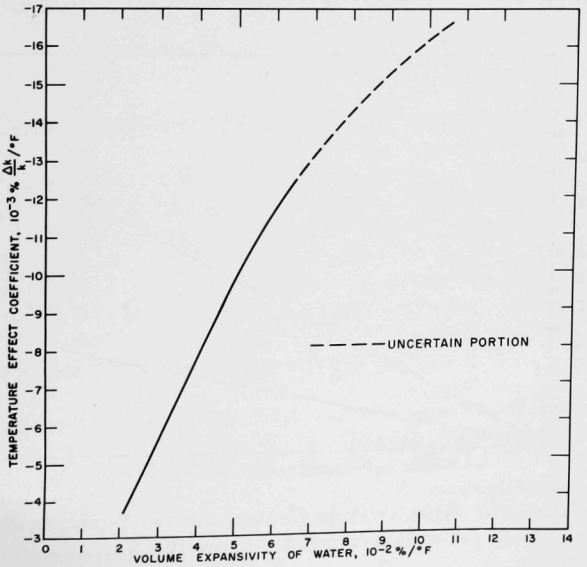

Fig. 55. Temperature-effect Coefficient of Reactivity vs. Volume Expansivity of Water for Core B-1D

between these two values are as follows: (a) the cores are somewhat different; (b) as mentioned in Section III.C.3.a, the value reported there includes some streaming effects caused by voids in the upper and lower reflectors; (c) the experiment of Section III did not include effects of void in the radial reflector; (d) the "lumped" void in the experiment of Section III probably had about the same effect on fast leakage as does a homogeneously distributed void, but the effects on thermal utilization, fast fission, and resonance escape may be appreciably different from those of a homogeneously distributed void; (e) the reactivity effect of a temperature change is not merely a result of changed moderator density, for the temperature change itself affects thermal utilization and neutron spectrum.

C. Boric Acid Effects

All boric acid concentrations were measured at room temperature and pressure, and all concentrations are given for these conditions. If the assumption is made that the reactivity worth of control rods is not changed by boric acid dissolved in the water, then the distinction disappears between boric acid reactivity effect and change in available excess reactivity caused by boric acid. With this assumption and with temperature corrections from Fig. 54, the data of Figs. 50 and 51 were analyzed to determine the reactivity in boric acid at 80°F and at 489°F as a function of boric acid concentration. The results are shown in Fig. 56. The reactivity controlled by boric acid appears to be very nearly proportional to concentration. The slope of the curve for 80°F is -0.55% $\Delta k/k$ per $g(H_3BO_3)/gal(H_2O)$, and for 489°F the slope is -0.22% $\Delta k/k$ per $g(H_3BO_3)/gal(H_2O)$.

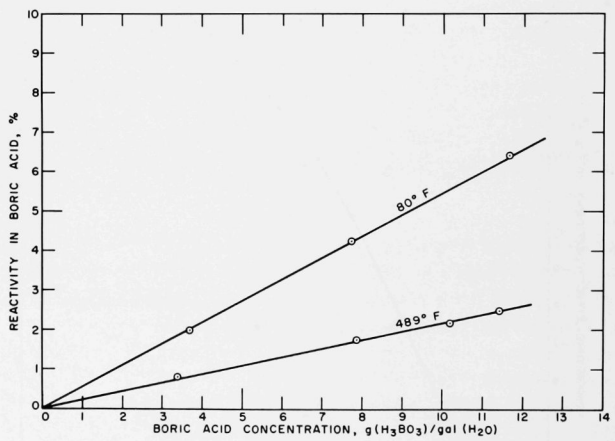

Fig. 56. Reactivity in Boric Acid vs. Boric Acid Concentration for Core B-1D

The decrease in density of reactor water to 0.79 g/cm^3 at 489°F is insufficient by itself to account for this decrease in boric acid worth. The reactivity worth of boric acid as a function of temperature is shown in Fig. 57. The marked decrease in boric acid worth with increasing temperature is not in accord with earlier experience;[7] since this effect is closely related to the decrease in control rod worth with increasing temperature, discussed above, the cause is also not clear.

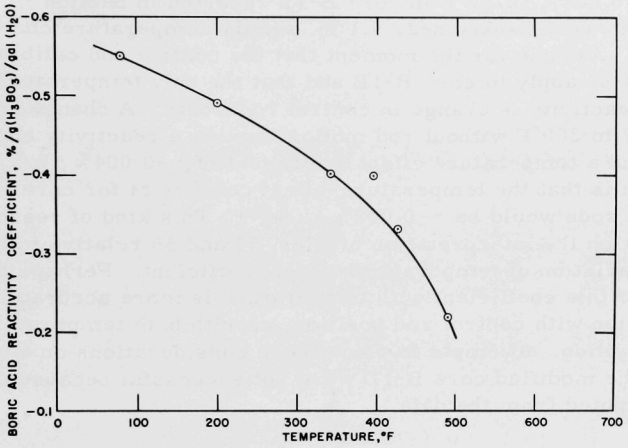

Fig. 57. Boric Acid Reactivity Coefficient vs. Temperature for Core B-1D

V. DISCUSSION OF TEMPERATURE AND VOID EFFECTS

In Section IV.B it is reported that a change from room temperature to 489°F in core B-1D caused a loss in available excess reactivity of 5.9% $\Delta k/k$. If it is assumed that this loss of reactivity due to change of temperature is caused only by decrease in moderator density, then the average void coefficient of available excess reactivity from 0% void to 20.7% void is -0.28% per % void. Calculated average void coefficients of available excess reactivity from 0% void to 15% void are -0.21% per % void at room temperature and -0.27% per % void at 489°F.[1]

If it is assumed that the temperature variation of the boric acid effect in core B-1A is given by Fig. 57, then the "essentially zero" temperature-effect coefficient with a concentration of 18.75 g(H_3BO_3)/gal(H_2O) reported in Section III.C.1.b requires correction for the temperature variation of boric acid worth. The correction is about -0.19% $\Delta k/k$, and the corresponding temperature-effect coefficient for core B-1A without control rods is about -0.009% $\Delta k/k$ per °F.

This result leads to at least two instructive considerations: (a) A temperature change from 79 to 101°F is involved in this temperature-effect coefficient, and the corresponding density change of water is about 0.385%. If it is assumed that the change in water density is the only mechanism by which reactivity is altered, then the void effect coefficient is about -0.49% $\Delta k/k$ per % void. This coefficient is not unreasonable in view of the measured coefficients in Section III.C.3. (b) For the temperature-effect coefficient of ~-0.004% $\Delta k/k/°F$ in core B-1B reported in Section III.C.1, the control rods were banked near 9.1 in. and the temperature changed from 67 to 94°F. Assume for the moment that the control rod calibration curves in Figs. 50-51 apply to core B-1B and that the only temperature mechanism affecting reactivity is change in control rod worth. A change from criticality at 77 to 200°F without rod motion implies a reactivity change of ~+0.50% and a temperature effect coefficient of ~+0.004% $\Delta k/k/°F$. The implication is that the temperature-effect coefficient for core B-1B without control rods would be ~-0.008% $\Delta k/k/°F$. This kind of reasoning casts some doubt on the interpretation of Figs. 54 and 55 relative to the temperature variation of temperature-effect coefficient. Perhaps the apparent variation of this coefficient with temperature is more accurately described as a variation with control rod position, or with both temperature and control rod position. Attempts to place these considerations on a quantitative basis for the modified core B-1D were not successful because of scatter of points computed from the data.

ACKNOWLEDGMENTS

The contributors to this report wish to express their appreciation to the following people whose diligent efforts and interest made the publication of this report possible:

D. H. Shaftman, consultant on reactor physics; R. S. Harding, E. Atkin, D. L. Birdsall, L. F. Karan, J. F. Kerr, L. K. Larson, L. R. Monson, B. J. Nelson, J. P. Newman, E. W. O'Neal, D. B. Sarutzki, and R. S. Woolf of the BORAX-V Operating Crew; J. L. Durney, a temporary Student Aide, for assistance with the flux-mapping experiments; S. L. Slate for numerical calculations, curve plotting, and flux-wire counting; C. Hendrix for assistance in data reduction; C. M. Ekelund, D. R. Greenwood, K. E. Tibbitts, and D. E. Whitney for preparation of the graphs, drawings, and diagrams; M. L. Ramshaw for stenographic services and proofreading; and W. P. Rosenthal for final editing.

REFERENCES

1. Design and Hazards Summary Report, BORAX-V, ANL-6302 (June 1961).

2. Juliano, J. O., and T. Kanai, Results of the BORAX-V Boiling Region Critical Experiments, ANL Hi-C Memo #37 (Sept 20, 1961).

3. Shaftman, D. H., Zero-power Experiments on the Argonne Low Power Reactor (ALPR), ANL-6078 (May 1961).

4. Reactor Physics Constants, ANL-5800.

5. Kirn, F. S., and J. I. Hagen, BORAX-V Exponential Experiment, ANL-6707 (April 1963).

6. Maxon, B. S., O. A. Schulze, and J. A. Thie, Reactivity Transients and Steady-state Operation of a Thoria-Urania-fueled Direct-cycle Light Water-boiling Reactor (BORAX-IV), ANL-5733 (Feb 1959).

7. Gallagher, J. M., Jr., et al., The Startup Experiment Program for the Yankee Reactor, YAEC-184 (June 1961).

8. Reactor Development Progress Report, November, 1962, ANL-6658.

9. Spano, A. H., et al., Self-limiting Power Excursion Tests of a Water-moderated Low-enrichment UO_2 Core in SPERT I, IDO-16751 (Feb 1962).

10. Reactor Development Progress Report, December, 1962, ANL-6672.